SPHERICALLY SYMMETRIC EINSTEIN-AETHER KANTOWSKI-SACHS COSMOLOGICAL MODELS WITH SCALAR FIELD

by

Amal Alhaddad

Submitted in partial fulfillment of the requirements
for the degree of Master of Science

at

Dalhousie University
Halifax, Nova Scotia
June 2016

Table of Contents

List of Tables

List of Figures

Abstract

In this thesis we first give a brief introduction to the application of dynamical systems to cosmology. This enables us to study spherically-symmetric cosmological models in Einstein-aether theory with a scalar field. The models depend on the time-like aether vector field through the expansion and shear scalars, and we focus on some special cases of the models. This leads to a compact phase space. From the evolution equations we obtain a three-dimensional dynamical system in terms of expansion-normalized variables. The aim of studying this system is to find the local stability of the equilibrium points of the dynamical system corresponding to physically realistic solutions. As an application we study spherically symmetric Einstein-aether Kantowski-Sachs cosmological models with a scalar field using the dynamical systems theory. In general, we found that there always exists an future attractor for the points ${}^{+}P_1$,${}^{\pm}P_2$,${}^{\pm}P_4$ for different values of the parameters $k > 0$ and $c > 0$ and $-\infty < \alpha < \infty$.

List of Abbreviations Used

IR limit	Infrared Limit of Horava Gravity
CMB	Cosmic Microwave Background
u_a	The Aether Velocity Vector Field
g_{ab}	The Metric Tensor
V	Potential
ρ	Energy Density
p	Pressure
DE	Differential Equation
ϕ	Scalar Field
θ	Expansion of the Aether
σ_+	Shear of the Aether
$\dot{u}^a$	Acceleration of the Aether
t	Time
k	Curvature Parameter
$a(t)$	Expansion Scale Factor
ds^2	The line element
A	Matrix
$R_1(x, a)$	The error term
$Df(a)$	Derivative Matrix
$\mathbf{e}^{tA}$	The Linear Flow
$\gamma(a)$	The Orbit

$\gamma^+(a)$	The Positive Orbit
J	Jordan Canonical Form
λ	Eigenvalue
$\Re e(\lambda_i)$	Real Part
FLRW	Friedmann-Lemaitre -Robertson-Walker
N	Non-negative Function
$\mu^\phi, p^\phi, q_1^\phi, \pi_+^\phi$	The Aether Energy Momentum Components
$\mathcal{L}_u$	The Einstein-Aether Lagrangian

Acknowledgements

First and foremost, I would like to thank Dr. Alan Coley, professor of Mathematics in the Department of Mathematics and Statistics, Dalhousie University, for his patience, guidance, and support in helping me improve my knowledge in different areas of mathematics. Also, I would like to thank Dr.David Iron, professor of Mathematics and the graduate coordinator in the Department of Mathematics and Statistics, Dalhousie University, for his guidance and support. I would like to thank Dr. Robert van den Hoogen, professor of Mathematics in the Department of Mathematics and Statistics, St. Francis Xavier University, for his patience, guidance, and valuable advices throughout the duration of this study. Special thanks go out to my parents (Masoud Al haddad and Saadah Saleh), my husband (Turki Alhadad), and all my sisters, brothers, and my friends for their support, love, and for providing me a good academic environment during the length of my study. Special thanks are extended to Ms.Bassemah Alhulaimi, PhD student in Applied Mathematics, Department of Mathematics and Statistics, for her guidance and support. Last but not least, I would like to thank our king of Saudi Arabia and the Saudi Cultural Bureau in Canada for their support and for giving me the chance to continue my studies abroad.

Chapter 1

Introduction

1.1 Application of Dynamical Systems in Cosmology

Dynamical systems are helpful in the study of the Universe on the largest scales, where galaxies are taken to be the constituents. Studies show that galaxies are distributed fairly uniformly, so we can assume that the cosmological models are spatially homogeneous and the Einstein field equations of General Relativity are ordinary differential equations. As a result, using dynamical systems theory we can study the qualitative features of such models.
Several models of early universe cosmology, including the Einstein-aether theory [1, 2] and the IR limit of Horava gravity [3, 4], break Lorentz invariance. There are some theories where the physical laws are measured to be the same for all observers that are moving uniformly with respect to each other. These are called the Lorentz invariant theories. When Einstein-aether theories are studied, it is assumed that the rest frame (which is usually chosen) matches with the Hubble law expansion of the universe and the CMB. On the other hand, it has been shown [5] that a cosmological rest frame does not exist, and as a result there is no point in assuming that the aether should match such a cosmological rest frame.

Einstein-aether theory joins General Relativity with the aether, a dynamic unit time-like vector field. An Einstein-aether solution is a Horava solution if the aether vector field is hyper-surface orthogonal. In Einstein-aether theory, the local time structure consists of the aether vector field u_a and the metric tensor g_{ab}. We can illustrate much of the physics of the early universe in conventional cosmology by knowing the impact of inflation on the Lorentz violation [6, 7]. In this thesis, we analyze the late time behaviour of the dynamics of Einstein-aether cosmological models. Researchers predict that in aether theory the Lorentz violation vector may be the reason for inflation without the scalar field potential, changing the dynamics of the chaotic inflationary

model [8–10].

1.2 Einstein-Aether Cosmology

Recently, the use of aether theories of gravity in cosmological models has become more popular in research. In [1, 11–15], an Einstein-aether gravity theory is improved with a Lorentz-violating dynamic field that conserves both locality and covariance with an additional aether vector field. The aether vector field will coincide with the cosmic frame and the expansion rate of the universe in an isotropic, homogeneous Friedmann universe, with the expansion scale factor $a(t)$ and the proper time t. The Einstein equations can be generalized by adding a stress tensor for the aether field which has the form:

$$\begin{aligned} T^{ae}_{ab} &= 2c_1(\nabla_a u^c \nabla_b u_c - \nabla^c u_a \nabla_c u_b) - 2[\nabla_c(u_{(a}J^c_{b)}) + \nabla_c(u^c J_{(ab)}) - \nabla_c(u_{(a}J^c_{b)})] \\ &\quad -2c_4 \dot{u}_a \dot{u}_b + 2\lambda u_a u_b + g_{ab}\mathcal{L}_u \end{aligned}$$

where

$$K^{ab}_{cd} \equiv c_1 g^{ab} g_{cd} + c_2 \delta^a_c \delta^b_d + c_3 \delta^a_d \delta^b_c + c_4 u^a u^b g_{cd},$$

$$J^a_m = -K^{ab}_{mn} \nabla_b u^n$$

$$\mathcal{L}_u \equiv -K^{ab}_{cd} \nabla_a u^c \nabla_b u^d.$$

We define new expressions $c_\theta = c_2 + (c_1 + c_3)/3$ and $c_\sigma = c_1 + c_3$ [36].

1.3 Self Interacting Scalar Field

If the universe contains a self-interaction potential V, which is dependent on a self-interacting scalar field ϕ, together with the expansion rate $\theta = \frac{3\dot{a}}{a} = 3H$, the modified stress tensor for the scalar field [1, 2] is given by

$$T_{ab} = \nabla_a \phi \nabla_b \phi - (\frac{1}{2}\nabla_c \phi \nabla^c \phi - V + \theta V_\theta) g_{ab} + \dot{V_\theta}(u_a u_b - g_{ab}) \tag{1.1}$$

where V_θ is the derivative of V with respect to θ. This corresponds to an effective fluid with energy density ρ^ϕ and pressure p^ϕ that can be expressed as follows:

$$\rho^\phi = \frac{1}{2}\dot{\phi}^2 + V - \theta V_\theta \quad \text{and} \quad p^\phi = \frac{1}{2}\dot{\phi}^2 - V + \theta V_\theta + \dot{V}_\theta.$$

The energy-momentum conservation law, or Klein-Gordon equation, is

$$\ddot{\phi} + \theta\dot{\phi} + V_\phi = 0, \tag{1.2}$$

the augmented Friedmann equation is

$$\frac{1}{3}\theta^2 = \rho^\phi + \frac{1}{2}\dot{\phi}^2 + V - \theta V_\theta - \frac{k}{a^2} \tag{1.3}$$

(where k is the curvature parameter and ρ^ϕ is the density of ordinary matter), and the Friedmann metric is defined by the line element

$$ds^2 = dt^2 - a^2(t)(\frac{dr^2}{1-kr^2} + r^2 d\vartheta^2 + r^2 \sin^2\vartheta d\varphi^2). \tag{1.4}$$

We then get the Raychaudhuri equation from differentiating the Friedmann equation.

1.4 Exponential potentials

Exponential potentials of the form $V = V_0 e^{-\lambda\phi}$ occur in higher dimensional frameworks, Kaluza-Klein theories, and super gravity [16–20]. Although in general relativity the exponential potential of the scalar field does not lead to exponential inflation [6, 7], if the potential is not too steep it can lead to a power law inflation. Ultimately, we restrict the steep potentials by using multiple fields in order to have assisted inflation [21–25]. A late time attractor is a scaling solution for exponential potentials with sufficiently flat potentials [26–30]. The dynamical system with negative exponential leads to rich physics, such as that which is found in Ekpyrotic behaviour [31, 32]. The main reason of using this kind of exponential potentials is that the dynamical system that results allows us to use dimensionless variables.

Chapter 2

Theory of Dynamical Systems

If we have a function $f : \mathbb{R}^n \to \mathbb{R}^n$ of class C^1, we can consider differential equations (DE's) of the form

$$x' = f(x), \tag{2.1}$$

where $x = (x_1(t), \cdots, x_n(t))$ is called the state space, a function of time, and $x' = \frac{dx}{dt}$. If f does not explicitly depend on t, the DE is called *autonomous*. Therefore, if f is linear then the DE is called *linear*, and is given by $f(x) = Ax$, where A is an $n \times n$ matrix of real numbers. In general, f is a non-linear function. The function f can be interpreted as a vector field, for each point $x \in \mathbb{R}^n$, we identify a vector $f(x) = (f_1(x), \ldots, f_n(x)) \in \mathbb{R}^n$.

We now give some important definitions and notations:
A *solution* of the DE defined above is a function $\psi : \mathbb{R} \to \mathbb{R}^n$ which satisfies the condition

$$\psi'(t) = f\big(\psi(t)\big) \tag{2.2}$$

for all $t \in \mathbb{R}$ in the domain of ψ. The orbits of the DE are the images of the solutions ψ. The tangent vector to the orbit of some solution ψ at $\psi(t)$ is given by $\psi'(t)$, satisfying (2.2), and so the vector f is tangent to such an orbit. A zero of the vector field is a point $a \in \mathbb{R}^n$ satisfying

$$f(a) = 0, \tag{2.3}$$

which is called an *equilibrium point* or *equilibrium point* of the DE. $\psi(t) = a$, for all $t \in \mathbb{R}$, is a solution of the DE if and only if a is a equilibrium point, since $\psi'(t) = 0 = f(a)$. Such a constant solution describes a *equilibrium state* of the physical system. It is necessary to examine the behaviour of the orbits of the DE in order to study the stability of equilibrium states near the equilibrium points. Since we are assuming f is

of class C^1, we have

$$f(x) = f(a) + Df(a)(x-a) + R_1(x,a), \tag{2.4}$$

with

$$\lim_{x\to a} \frac{||R_1(x,a)||}{||x-a||} = 0$$

Here, $R_1(x,a)$ is called the *error term*, and $Df(a)$ is the $n \times n$ derivative matrix of f defined by

$$Df(x) = \left(\frac{\partial f_i}{\partial x_j}\right), \quad i,j = 1, \cdots, n. \tag{2.5}$$

If $a \in \mathbb{R}^n$ is such that $f(a) = 0$, then using (2.4) we can rewrite (2.1) as

$$x' = f(x) = Df(a)(x-a) + R_1(x,a). \tag{2.6}$$

The *linearization* of the DE (2.1) is given by the linear DE

$$u' = Df(a)u$$

for the equilibrium point $a \in \mathbb{R}^n$. Since $f(x) \approx Df(a)(x-a)$ for x near a equilibrium point a, solutions of such a linearization will in general approximate the solutions of the original non-linear DE near the equilibrium points.

2.1 Linear Autonomous Differential Equations

There is a unique solution curve for the linear DE

$$x' = Ax, \qquad x(0) = a \in \mathbb{R}^n, \tag{2.7}$$

where

$$x(t) = \mathbf{e}^{tA}a \qquad \text{for all } t \in \mathbb{R}, \tag{2.8}$$

where $\mathbf{e}^{tA}$ maps $a \to e^{ta}a$ for all $t \in \mathbb{R}$ and $a \in \mathbb{R}^n$, and A is an $n \times n$ real matrix. The *linear flow* of the DE is a one-parameter family of linear maps, and is denoted by

$$\mathrm{g}^t = \mathbf{e}^{tA}. \tag{2.9}$$

The properties

$$\mathrm{g}^0 = I \quad \text{and} \quad \mathrm{g}^{t+s} = \mathrm{g}^t \circ \mathrm{g}^s, \quad \forall\ t, s \in \mathbb{R}, \tag{2.10}$$

hold for both the linear and non-linear flow. Thus the linear flow $\{e^{tA}\}_{t\in\mathbb{R}}$ has a group structure under the composition of maps. The evolution of the dynamical system in terms of time can be described by the flow in terms of the physical system. The *orbits* are subsets of $\mathbb{R}^n$ divided by the flow of the DE, and are denoted by:

$$\gamma(a) = \left\{\mathrm{g}^t a | t \in \mathbb{R}\right\}. \tag{2.11}$$

This is called the orbit of the DE through a and is the image of the solution curve $x(t) = e^{tA}a$. As a result of the uniqueness of the solution, either of the properties:

$$\gamma(a) = \gamma(b) \ \text{ or } \gamma(a) \cap \gamma(b) = \emptyset$$

hold, for all $a, b \in \mathbb{R}^n$. A set S is called an invariant set if for any point $a \in S$ the orbit through a remains in S that is $\gamma(a) \in S$.

The orbits of the DE can be classified as follows :

1. If $\mathrm{g}^t a = a$ for all $t \in \mathbb{R}$, then $\gamma(a)$ is a *point orbit.*
2. If there exists a $T > 0$ such that $\mathrm{g}^T a = a$, then $\gamma(a)$ is a *periodic orbit.*
3. If $g^t a \neq a$ for all $t \neq 0$, then $\gamma(a)$ is a *non-periodic orbit.*

Definitions

1. Given a linear DE $x' = Ax$ in $\mathbb{R}^n$, we can define a new function $y = Px$, P is a non-singular matrix. Let $\tau = kt$ be a new variable, with $k > 0$. It follows that $y' = By$, where $B = \frac{1}{k} P\, A\, P^{-1}$. Moreover, the two linear dynamical systems $x' = Ax$ and $x' = Bx$, where $A = kP^{-1}\, B\, P$, are *linearly equivalent.*

   (The condition $A = kP^{-1}\, B\, P$ means that the linear map P maps each orbit of the flow e^{tA} to an orbit of the flow e^{tB}.)

2. We can say that the two linear flows e^{tA} and e^{tB} on $\mathbb{R}^n$ are linearly equivalent if there exists a non-singular matrix P and a parameter $k > 0$ such that $\forall t \in \mathbb{R}, P\, \mathbf{e}^{tA} = \mathbf{e}^{ktB}\, P$.

From these definitions we can classify the Jordan Canonical forms for any 2×2 real matrix (A) as follows:

1. There exists a matrix P such that $J = P\,A\,P^{-1}$ if A has two real independent eigenvalues, and so the flow is then denoted by e^{tJ}, where

$$J = \begin{bmatrix} \lambda_1 & 0 \\ 0 & \lambda_2 \end{bmatrix}, \quad e^{tA} = \begin{bmatrix} \mathbf{e}^{\lambda_1 t} & 0 \\ 0 & \mathbf{e}^{\lambda_2 t} \end{bmatrix}.$$

   The eigenvectors are $e_1 = (1,0)^T$ and $e_2 = (0,1)^T$. The resulting solution is $y(t) = \mathbf{e}^{tJ}b$, $b \in \mathbb{R}^2$ (i.e., $y_1 = \mathbf{e}^{\lambda_1 t}b_1$ and $y_2 = \mathbf{e}^{\lambda_2 t}b_2$). Note that the orbits of the DE for the non-zero eigenvalues are given by

$$\left[\frac{y_1}{b_1}\right]^{\frac{1}{\lambda_1}} = \left[\frac{y_2}{b_2}\right]^{\frac{1}{\lambda_2}}.$$

2. If there is one real eigenvalue of A, then there exists a matrix P such that $J = P\,A\,P^{-1}$, and the flow is given by e^{tJ}, where

$$J = \begin{bmatrix} \lambda & 0 \\ 0 & \lambda \end{bmatrix}, \quad e^{tA} = e^{\lambda t}\begin{bmatrix} 1 & t \\ 0 & 1 \end{bmatrix}$$

   The eigenvector is given by $e_1 = (1,0)^T$. Note that the orbits of the DE for the non-zero eigenvalues are of the form

$$y_1 = y_2\left[\frac{b_1}{b_2} + \frac{1}{\lambda}\log\frac{y_2}{y_1}\right].$$

3. If the eigenvalues of A are complex of the form $\alpha + i\beta$, then there exists a matrix P such that $J = P\,A\,P^{-1}$, where

$$J = \begin{bmatrix} \alpha & \beta \\ -\alpha & \beta \end{bmatrix}.$$

We adopt the polar coordinates (r,θ), with $y_1 = r\cos\theta$ and $y_2 = r\sin\theta$, in order to simplify the calculation of orbits. Then the DE becomes $r' = \alpha r$ and $\theta' = -\beta$, implying that $\frac{dr}{d\theta} = -\frac{\alpha}{\beta}r$. Without loss of generality, we can assume $\beta > 0$, since the DE is invariant under the changes $(\beta, y_1) \to (-\beta, -y_1)$. Thus, $\lim_{t\to\infty}\theta = -\infty$.

2.2 Topological Equivalence of Linear Flows

Linear equivalence acts as a filter; the flow is limited by the number of distinct eigenvectors of the DE. Hence, near the equilibrium points the linear equivalence of the DE can distinguish the behaviour of the orbits. For example, the orbits in the three Jordan Canonical forms approach the origin as $t \to \infty$. On the other hand, we can study the long time behaviour of the DE by eliminating more features.

Definitions

1. *A homeomorphism* on $\mathbb{R}^n$ is a non-linear map $h : \mathbb{R}^n \to \mathbb{R}^n$, where h is one to one and onto, and h^{-1} is continuous. The orbits of one of the flows can be mapped onto the orbits of the simplest flow using a homeomorphism.

2. Two linear flows $\mathbf{e}^{tA}$ and $\mathbf{e}^{tB}$ on $\mathbb{R}^n$ are *topologically equivalent* if there exists a homeomorphism h on $\mathbb{R}^n$ and a positive constant k such that $h\left(\mathbf{e}^{tA}x\right) = \mathbf{e}^{ktB}h(x)$ for all $x \in \mathbb{R}^n$ and for all $t \in \mathbb{R}$.

If the real part of the eigenvalues are all non zero (i.e., $\Re e(\lambda_i) \neq 0, \quad i = 1, 2$), then the flow is called *hyperbolic*. In fact, any hyperbolic linear flow in $\mathbb{R}^2$ is topologically equivalent to the linear flow e^{tA}, where A is one of the following matrices:

$$A = \begin{pmatrix} -1 & 0 \\ 0 & -1 \end{pmatrix} (sink), A = \begin{pmatrix} 1 & 0 \\ 0 & 1 \end{pmatrix} (source), A = \begin{pmatrix} -1 & 0 \\ 0 & 1 \end{pmatrix} \text{ (saddle).}$$

2.3 Linear Stability

It is important to determine whether a physical system which is disturbed from an equilibrium state remains close to, or approaches, the equilibrium points as $t \to \infty$.

Further definitions

1. A equilibrium point of the DE is called *stable* if for all neighbourhoods U of 0, there exists a neighbourhood V of 0 such that $\mathrm{g}^t V \subseteq U$ for all $t \geq 0$, where $\mathrm{g}^t = (\mathbf{e}^{tA})$ is the flow of the DE.

2. A equilibrium point is called *asymptotically stable* if the equilibrium point is stable, and if for all $x \in V$, $\lim_{t\to\infty} \|\mathrm{g}^t x\| = 0$.

Note if $A \in M_n(\mathbb{R})$ we will see that

$$\lim_{t\to\infty} \mathbf{e}^{tA}a = 0 \qquad \text{for all } a \in \mathbb{R}^n \tag{2.12}$$

if and only if $\Re e(\lambda) < 0$ for all eigenvalues of A. This implies that $(0,0)$ is a sink in $\mathbb{R}^n$, if the solutions $x(t)$ of the DE approach the equilibrium points $(0,0)$ in the long term behaviour of the dynamical system. On the other hand, if we replace A by $-A$ and t by $-t$, we obtain that $\Re e(\lambda) > 0$ for all eigenvalues which are called a *source* in $\mathbb{R}^n$.

2.4 Non-Linear Differential Equations

For non linear DE it is difficult to write down the flow explicitly, so the main aim of the dynamical system analysis is to show the qualitative properties of a non-linear flow without knowing the exact form of the flow.

We shall consider the DE $x' = f(x)$, where f is of class C^1. It has a unique maximal solution satisfying $\psi_a(0) = a$. The flow of the DE is defined by the one-parameter family of maps $\{\mathrm{g}^t\}_{t\in\mathbb{R}}$ such that $\mathrm{g}^t : \mathbb{R}^n \to \mathbb{R}^n$ and $\mathrm{g}^t a = \psi_a(t)$, for all $a \in \mathbb{R}^n$. The flow $\{\mathrm{g}^t\}$ is defined by

$$\mathrm{g}^t a = \psi_a(t), \tag{2.13}$$

in terms of the solution function $\psi_a(t)$ of the DE .

Here, $\gamma(a)$, is the notation for the *orbit* through a and is defined as

$$\gamma(a) = \left\{ x \in \mathbb{R}^n \middle| x = \mathrm{g}^t a, \text{ for all } t \in \mathbb{R} \right\}. \tag{2.14}$$

Furthermore, orbits for non-linear flows can be classified into three types (as for linear flows): *point orbits*, *periodic orbits*, and *non-periodic orbits.*

A *positive orbit through* a, denoted by $\gamma^+(a)$, which we sometimes work with, is defined as

$$\gamma^+(a) = \left\{ x \in \mathbb{R}^n \middle| x = \mathrm{g}^t a, \text{ for all } t \geq 0 \right\}. \tag{2.15}$$

2.5 Linearization and the Hartman-Grobman Theorem

The Hartman-Grobman theorem plays a significant role in dynamical systems theory because it is useful to study the behavior of the stability of any dynamical system near the equilibrium points. Let us state the theorem in general:

Theorem 1. *Hartman-Grobman Theorem: Let $\bar{x}$ be a equilibrium point of the DE $x' = f(x)$ in $\mathbb{R}^n$, where $f : \mathbb{R}^n \to \mathbb{R}^n$ is a continuously differentiable map. If all of the eigenvalues of the derivative matrix $Df(\bar{x})$ satisfy $\Re e(\lambda) \neq 0$, then there is a homeomorphism $h : U \to \bar{U}$ of a neighbourhood U of $0 \in \mathbb{R}$ onto a neighbourhood $\bar{U}$ of $\bar{x}$ which maps orbits of the linear flow $\mathbf{e}^{tDf(\bar{x})}$ onto orbits of the non-linear flow g^t of the DE, preserving the parameter t.*

In particular, if $\bar{x}$ is a *hyperbolic equilibrium point* then the flow of the DE $x' = f(x)$ and the flow of its linearization $u' = Df(\bar{x})u$ are *locally* topologically equivalent.
Furthermore, if $\bar{x}$ is a equilibrium point of the DE, and the real parts of the eigenvalues of the matrix $Df(\bar{x})$ are all non-zero, then we can study its stability: if the real parts of the eigenvalues are all negative, the equilibrium point is called a sink; if all $Re(\lambda) > 0$, it is called a source. Otherwise, if one eigenvalue is positive and the other negative, it is a saddle point.

2.6 Higher Dimensions

Let give some important definitions:
Hyperbolic equilibrium point: if the real parts of the eigenvalues of the matrix $Df(\bar{x})$ are non-zero, the equilibrium point of a non-linear DE is said to be hyperbolic.
Non-hyperbolic equilibrium point: For a one- parameter family of equilibrium points there is at least one eigenvalue which has a zero real part for any equilibrium point in DE, but if all other eigenvalues have a non-zero real part, all points in the set are called non-hyperbolic.
In higher dimensions ($n > 2$) many new features are possible, and the Hartman Grobman Theorem can be applied if the equilibrium point is hyperbolic. Otherwise, we use the normally hyperbolic method if the equilibrium point is non- hyperbolic by identify the signs of the other eigenvalues for a curve, in the remaining $n - 1$ directions.

Note: all the information in this section is taken from [33].

Chapter 3

Spherically Symmetric Einstein-Aether Kantowski-Sachs Cosmological Models with a Scalar Field

The spherically-symmetric cosmological models in Einstein-aether theory are constructed containing a scalar field, in which the exponential self-interaction potential depends on the time-like aether vector field through the expansion and shear scalars. The derivation of the evolution equations in terms of expansion-normalized variables are presented below, which reduce to a dynamical system. The local stability of some of the equilibrium points of the dynamical system will be investigated in the next chapter.

3.1 Kantowski-Sachs Models

The Kantowski-Sachs models are spatially homogeneous, spherically symmetric cosmological models that have four Killing vectors, the fourth being ∂_x [35]. In coordinates adapted to the symmetries of the models, the metric can be written in the following form:

$$ds^2 = -N(t)^2 dt^2 + (e_1{}^1(t))^{-2} dx^2 + (e_2{}^2(t))^{-2}(d\vartheta^2 + \sin^2\vartheta d\varphi^2). \tag{3.1}$$

N is a non -negative function of t, which under a time rescaling can be set to one. It is assumed here that the aether field is invariant under the same symmetries as the metric, and therefore is aligned with the symmetry adapted time coordinate. The velocity vector of aether is assumed to satisfy $u^a u_a = -1$ [36]. The expansion scalar is determined via $\theta = \nabla_a u^a$, and the shear scalar is determined via $6\sigma_+^2 = \nabla_a u^b \nabla_b u^a - \frac{1}{3}\theta^2$. The vorticity and acceleration of the aether are zero [34].

3.2 Scalar Field Potential

The scalar field potential $V(\phi, \theta, \sigma_+)$ is assumed to be an exponential function of the scalar field and depends linearly on both the expansion and the shear of the Aether.

Consider the scalar field potential of the form

$$V(\phi,\theta,\sigma_+) = a_1 e^{-2k\phi} + a_2\theta e^{-k\phi} + a_3\sigma_+ e^{-k\phi}, \tag{3.2}$$

in which case

$$\mu^\phi = \tfrac{1}{2}\mathbf{e}_0(\phi)^2 + a_1 e^{-2k\phi}, \tag{3.3}$$

$$p^\phi = \tfrac{1}{2}\mathbf{e}_0(\phi)^2 - a_1 e^{-2k\phi} - k a_2 \mathbf{e}_0(\phi) e^{-k\phi} - a_3\sigma_+ e^{-k\phi}, \tag{3.4}$$

$$q_1^\phi = 0, \tag{3.5}$$

$$\pi_+^\phi = \frac{a_3}{6}\big(\theta - k\mathbf{e}_0(\phi)\big)e^{-k\phi}. \tag{3.6}$$

The aether energy components are derived in [34] where we replace $\mathbf{e}_1(\phi) = 0$ and $\dot{u} = 0$. The constants a_1, a_2 and a_3 are defined such that the potential $V(\theta,\phi,\sigma)$ can be assumed to be a positive definite. We shall assume that $a_1 > 0$ but allow a_2 and a_3 to be either positive or negative.

3.3 Evolution Equations

The evolution equations for the aether-Kantowski-Sachs models with a scalar field are:

$$\mathbf{e}_0({e_1}^1) = -\tfrac{1}{3}(\theta - 6\sigma_+){e_1}^1, \tag{3.7a}$$

$$\mathbf{e}_0(K) = -\tfrac{2}{3}(\theta + 3\sigma_+)K, \tag{3.7b}$$

$$\mathbf{e}_0(\theta) = -\tfrac{1}{3}\theta^2 - 6\left(\frac{1-2c_\sigma}{1+3c_\theta}\right)\sigma_+^2 + \frac{1}{1+3c_\theta}\big(-\mathbf{e}_0(\phi)^2 + a_1 e^{-2k\phi} + \tfrac{3}{2}a_2 k e^{-k\phi}\mathbf{e}_0(\phi) + \tfrac{3}{2}a_3\sigma_+ e^{-k\phi}\big), \tag{3.7c}$$

$$\mathbf{e}_0(\sigma_+) = -\theta\sigma_+ + \frac{1}{6(1-2c_\sigma)}\big(a_3\theta e^{-k\phi} - a_3 k\mathbf{e}_0(\phi)e^{-k\phi} - 2K\big), \tag{3.7d}$$

$$\mathbf{e}_0(\mathbf{e}_0(\phi)) = -\theta\mathbf{e}_0(\phi) + 2k a_1 e^{-2k\phi} + (a_2\theta + a_3\sigma_+)k e^{-k\phi}, \tag{3.7e}$$

with the following constraint:

$$K + \tfrac{1}{3}(1+3c_\theta)\theta^2 = 3(1-2c_\sigma)\sigma_+^2 + \tfrac{1}{2}\mathbf{e}_0^2(\phi) + a_1 e^{-2k\phi}. \tag{3.8}$$

where c_σ and c_θ are parameters (see chapter one). All evolution and constraint equations are derived in [34].

3.4 Dimensionless Variables

In order to simplify the analysis the following normalized variables (which are bounded for $1-2c_\sigma \geq 0$), are chosen:

$$x=\frac{\mathbf{e}_0(\phi)}{\sqrt{2}D},\quad y=\frac{\sqrt{3}\sigma_+}{D},\quad z=\frac{\sqrt{K}}{D},\quad Q=\frac{\theta}{\sqrt{3}D},\quad W=\frac{e^{-k\phi}}{D}, \tag{3.9}$$

where

$$D=\sqrt{K+\frac{\theta^2}{3}}, \tag{3.10}$$

and the new time variable

$$f'=\frac{1}{D}e_0(f) \tag{3.11}$$

is defined. To further simplify the model the following parameter is defined

$$c^2=(1-2c_\sigma).$$

Thus, the evolution equations for the aether-Kantowski-Sachs model with a scalar field can be written with the new variables defined in (3.9):

$$\begin{aligned}
\mathbf{e}_0(K) &= -\tfrac{2}{3}\sqrt{3}(Q+y)z^2D^4, && (3.12a)\\
\mathbf{e}_0(\theta) &= D^3\Bigg[-Q^2+\frac{1}{1+3c_\theta}\Bigg(-2c^2y^2-2x^2+a_1W^2 \\
&\quad +\frac{3\sqrt{2}}{2}a_2kxW+\frac{3}{2\sqrt{3}}a_3Wy\Bigg)\Bigg], && (3.12b)\\
\mathbf{e}_0(\sigma_+) &= D^3\left[-Qy+\frac{1}{6c^2}\left(\sqrt{3}a_3QW-\sqrt{2}a_3kWx-2z^2\right)\right], && (3.12c)\\
\mathbf{e}_0(\mathbf{e}_0(\phi)) &= D^3\left[-\sqrt{6}Qx+2ka_1W^2+\sqrt{3}\left(a_2Q+\frac{a_3}{3}y\right)kW\right], && (3.12d)
\end{aligned}$$

with the following constraints:

$$z^2+(1+3c_\theta)Q^2=c^2y^2+x^2+a_1W^2,$$

$$z^2+Q^2=1.$$

The differential equation for each of the normalized variables in (3.9) and with respect to the new time vairable in (3.11) is calculated Thus, the following five dimensional

dynamical system results [34]:

$$
\begin{aligned}
x' &= -\frac{2\sqrt{3}}{3}Qx + \sqrt{2}ka_1W^2 + \frac{\sqrt{3}}{\sqrt{2}}kW\left(a_2Q + \frac{a_3}{3}y\right) - \frac{\sqrt{3}xQ}{3(1+3c_\theta)} \\
&\quad \left[-2c^2y^2 - 2x^2 + a_1W^2 + \frac{\sqrt{3}}{2}a_3yW \right. \\
&\quad \left. + \frac{3\sqrt{2}}{2}a_2kWx\right] + \frac{\sqrt{3}}{3}xz^2y, \qquad (3.13a) \\
y' &= -\sqrt{3}Qy + \frac{\sqrt{3}}{3}yz^2(Q+y) + \frac{\sqrt{3}}{3}yQ^3 \\
&\quad + \frac{\sqrt{3}}{6c^2}\left[-2z^2 + \sqrt{3}a_3QW - \sqrt{2}a_3kWx\right] - \frac{\sqrt{3}yQ}{3(1+3c_\theta)} \\
&\quad \left[-2c^2y^2 - 2x^2 + a_1W^2 + \frac{\sqrt{3}}{2}a_3yW + \frac{3\sqrt{2}}{2}a_2kWx\right] \qquad (3.13b) \\
z' &= \frac{-\sqrt{3}zQ}{\sqrt{3}}\left[Qy + \frac{1}{1+3c_\theta}\left(- 2c^2y^2 - 2x^2 + a_1W^2 + \frac{\sqrt{3}}{2}a_3yW \right.\right. \\
&\quad \left.\left. + \frac{3\sqrt{2}}{2}a_2kWx\right)\right], \qquad (3.13c) \\
Q' &= \frac{z^2}{\sqrt{3}}\left[Qy + \frac{1}{1+3c_\theta}\left(- 2c^2y^2 - 2x^2 + a_1W^2 + \frac{\sqrt{3}}{2}a_3yW \right.\right. \\
&\quad \left.\left. + \frac{3\sqrt{2}}{2}a_2kWx\right)\right], \qquad (3.13d) \\
W' &= W\left[-\sqrt{2}kx + \frac{\sqrt{3}}{3}(Q+y) - \frac{\sqrt{3}}{3}Q^2y - \frac{\sqrt{3}Q}{3(1+3c_\theta)} \right. \\
&\quad \left.\left(- 2c^2y^2 - 2x^2 + a_1W^2 + \frac{3\sqrt{2}}{2}a_2kWx + \frac{\sqrt{3}}{2}a_3yW\right)\right]. \qquad (3.13e)
\end{aligned}
$$

The variables (3.9) are constrained by the following relations:

$$-3c_\theta Q^2 + x^2 + c^2y^2 + a_1W^2 = 1, \qquad (3.14a)$$

$$Q^2 + z^2 = 1. \qquad (3.14b)$$

The restrictions (3.14a), (3.14b) and the dynamical system (3.13) allow the elimination of z globally, but do not allow the elimination of x globally. This leads to a four-dimensional dynamical system with one constraint. However, the substitution for x

locally can be done, via

$$x = \epsilon\sqrt{1 - c^2y^2 + 3c_\theta Q^2 - a_1W^2}, \tag{3.15}$$

where $\epsilon = \pm 1$, obtaining two copies (one for each value of ϵ) of the dynamical system [34].

$$\begin{aligned}
y' &= Qy\Bigg[-\frac{2}{\sqrt{3}} - \frac{\sqrt{3}}{3}yQ - \frac{\sqrt{3}}{3(1+3c_\theta)}\Bigg(- 2 - 6c_\theta Q^2 + 3a_1W^2 \\
&\quad + \frac{3\epsilon\sqrt{2}}{2}a_2kW\sqrt{1 + 3c_\theta Q^2 - c^2y^2 - a_1W^2} + \frac{\sqrt{3}}{2}a_3yW\Bigg)\Bigg] \\
&\quad + \frac{\sqrt{3}}{3}\Bigg[y^2 + \frac{1}{2c^2}\Bigg(- 2(1-Q^2) + \sqrt{3}a_3QW \\
&\quad - \sqrt{2}\epsilon a_3kW\sqrt{1 + 3c_\theta Q^2 - c^2y^2 - a_1W^2}\Bigg)\Bigg], \qquad (3.16a) \\
Q' &= \frac{(1-Q^2)}{\sqrt{3}}\Bigg[Qy + \frac{1}{1+3c_\theta}\Bigg(- 2 - 6c_\theta Q^2 + 3a_1W^2 \\
&\quad + \frac{3\epsilon\sqrt{2}}{2}a_2kW\sqrt{1 - c^2y^2 - a_1W^2 + 3c_\theta Q^2} + \frac{\sqrt{3}}{2}a_3yW\Bigg)\Bigg], \qquad (3.16b) \\
W' &= W\Bigg[-\epsilon\sqrt{2}k\sqrt{1 + 3c_\theta Q^2 - c^2y^2 - a_1W^2} - \frac{\sqrt{3}}{3}Q^2y \\
&\quad + \frac{\sqrt{3}}{3}(Q+y) - \frac{\sqrt{3}Q}{3(1+3c_\theta)}\Bigg(- 2 + 3a_1W^2 - 6c_\theta Q^2 \\
&\quad + \frac{\sqrt{3}}{2}a_3yW + \frac{3\epsilon\sqrt{2}}{2}a_2kW\sqrt{1 - c^2y^2 - a_1W^2 + 3c_\theta Q^2}\Bigg)\Bigg]. \qquad (3.16c)
\end{aligned}$$

3.5 Special Case

Let us assume (from [34]) that $3c_\theta \equiv c_1 + 3c_2 + c_3 = 0$ and $a_3 = 0$. This leads to a compact phase space. Note that the variables y, Q and W are bounded by the conditions $y \in [\frac{-1}{c}, \frac{1}{c}]$, $Q \in [-1, 1]$, and $W \in [0, \frac{1}{\sqrt{a_1}}]$ which were obtained from equation (3.14). Also a_1, c, k are assumed to be positive numbers, while a_2 can be a negative or positive number. The evolution equations from (3.16) for the Kantowski-Sachs Aether

models contaning an interacting scalar field simplify, and lead to the three-dimensional dynamical system:

$$
\begin{aligned}
y' &= \frac{\sqrt{3}}{3}y\left[y - Q\left(yQ + 3a_1W^2 + \epsilon\frac{3\sqrt{2}}{2}a_2kW\sqrt{1-c^2y^2-a_1W^2}\right)\right] \\
&\quad -\frac{\sqrt{3}(1-Q^2)}{3c^2}, \qquad (3.17a)\\
Q' &= \frac{(1-Q^2)}{\sqrt{3}}\left[Qy - 2 + 3a_1W^2 + \epsilon\frac{3\sqrt{2}}{2}a_2kW\sqrt{1-c^2y^2-a_1W^2}\right], \qquad (3.17b)\\
W' &= W\left[\frac{\sqrt{3}}{3}y(1-Q^2) + \sqrt{3}Q(1-a_1W^2)\right. \\
&\quad \left. +\epsilon k\sqrt{1-c^2y^2-a_1W^2}\left(-\sqrt{2} - \frac{a_2\sqrt{6}}{2}QW\right)\right], \qquad (3.17c)
\end{aligned}
$$

with the following local definition for the following variable x

$$x = \epsilon\sqrt{1-c^2y^2-a_1W^2}$$

where $\epsilon = \pm 1$. This is the system which we will study in next chapter.

Chapter 4

The Dynamical System

Define a new parameter $\alpha = \frac{a_2}{\sqrt{a_1}}$ and a new variable

$$V = \sqrt{a_1}W. \tag{4.1}$$

Rewriting system (3.17) we obtain the new dynamical system which only depends on three parameters α , c and k , where $\epsilon = \pm 1$. :

$$\begin{aligned}
Q' &= \frac{(1-Q^2)}{\sqrt{3}}\left[Qy - 2 + 3V^2 + \epsilon\frac{3\sqrt{2}}{2}\alpha k V\sqrt{1-c^2y^2-V^2}\right], && \text{(4.2a)}\\
y' &= \frac{\sqrt{3}}{3}y\left[y - Q\left(yQ + 3V^2 + \epsilon\frac{3\sqrt{2}}{2}\alpha k V\sqrt{1-c^2y^2-V^2}\right)\right]\\
&\quad -\frac{\sqrt{3}(1-Q^2)}{3c^2}, && \text{(4.2b)}\\
V' &= V\left[\frac{\sqrt{3}}{3}y(1-Q^2) + \sqrt{3}Q(1-V^2)\right.\\
&\quad \left.+\epsilon k\sqrt{1-c^2y^2-V^2}\left(-\sqrt{2} - \frac{\alpha\sqrt{6}}{2}QV\right)\right], && \text{(4.2c)}
\end{aligned}$$

4.1 The Equilibrium Points

4.1.1 Equilibrium Points ($V = 0$):

The following table is a summary of the equilibrium points of the system (4.2) in the $V = 0$ set, which is a two dimensional invariant set of the dynamical system.

Note: We indicate the equilibrium points in the case of $\epsilon = 1$ by a $^+$ superscript on the left corner of the point, as in ${}^+P_1$, and ${}^-P_1$ for the case where $\epsilon = -1$, y^* is a parameter and hence the curves $P^*_{1,2}$ represent lines of equilibrium points.

Eq Pt	y	Q	V	Existence Condition
P_1^*	y^*	$+1$	0	$-\frac{1}{c} \leq y^* \leq \frac{1}{c}$ where $c > 0$
P_2^*	y^*	-1	0	$-\frac{1}{c} \leq y^* \leq \frac{1}{c}$ where $c > 0$
P_3	$\frac{1}{c}$	$2c$	0	$0 < c < \frac{1}{2}$
P_4	$-\frac{1}{c}$	$-2c$	0	$0 < c < \frac{1}{2}$

Table 4.1: Equilibrium points for the system (4.2) for both cases $\epsilon = \pm 1$, and their conditions of existence in the V=0 invariant set.

4.1.2 Equilibrium Points ($y = 0$, $Q^2 = 1$)

The flat FLRW models are contained in the one dimensional invariant sets $y = 0$, $Q = \pm 1$. The substitution of $y = 0, Q = \pm 1$, results in a zero for the first two equations of the dynamical system (4.2). Therefore, only the third equation in (4.2) is needed for determining the equilibrium points in the invariant set. When $y = 0, Q = \pm 1$, a non-linear equation is obtained in V as follows:

$$\sqrt{3}Q(1 - V^2) = \epsilon \frac{\sqrt{2}}{2} k \sqrt{1 - V^2} \left(2 + \alpha\sqrt{3}QV\right). \tag{4.3}$$

We can see easily that $V = 1$ is an equilibrium point for the above equation, then, other equilibrium points can be found by assuming $V \neq 1$ and dividing (4.3) by $\sqrt{1 - V^2}$, we obtain

$$\sqrt{3}Q\sqrt{1 - V^2} = \epsilon \frac{\sqrt{2}}{2} k \left(2 + \alpha\sqrt{3}QV\right), \tag{4.4}$$

where as usual $Q^2 = 1$ and $\epsilon^2 = 1$. Then, by squaring (4.4), we get

$$3(1 - V^2) = k^2 \left(\sqrt{2} + \frac{\alpha\sqrt{6}}{2} QV\right)^2. \tag{4.5}$$

The resulting quadratic equation results after doing some algebraic manipulations:

$$3V^2(\alpha^2 k^2 + 2) + 4\sqrt{3}\alpha k^2 QV + 2(2k^2 - 3) = 0, \tag{4.6}$$

which has two solutions for V as functions of (α, k, Q), given by

$$V_{1,2} = \frac{-2\sqrt{3}\alpha Q k^2 \pm \sqrt{b}}{3\alpha^2 k^2 + 2},$$

where b is defined by

$$b = 18k^2\alpha^2 + 36 - 24k^2.$$

Therefore, there is a maximum of four solutions for equation (4.5), two for $Q = 1$, which are P_7 and P_8, and two for $Q = -1$, which are P_9 and P_{10}.
Note: for additional analysis for these points (P_7 to P_{10}) see [34].

Eq Pt	y	Q	V
P_5	0	1	1
P_6	0	-1	1
P_7	0	1	$V_7 = \frac{-2\sqrt{3}\alpha k^2+\sqrt{18(\alpha^2k^2+2)-24k^2}}{3(\alpha^2k^2+2)}$
P_8	0	-1	$V_8 = \frac{2\sqrt{3}\alpha k^2+\sqrt{18(\alpha^2k^2+2)-24k^2}}{3(\alpha^2k^2+2)}$
P_9	0	1	$V_9 = \frac{-2\sqrt{3}\alpha k^2-\sqrt{18(\alpha^2k^2+2)-24k^2}}{3(\alpha^2k^2+2)}$
P_{10}	0	-1	$V_{10} = \frac{2\sqrt{3}\alpha k^2-\sqrt{18(\alpha^2k^2+2)-24k^2}}{3(\alpha^2k^2+2)}$

Table 4.2: FLRW equilibrium points of the system (4.2) for both cases $\epsilon = \pm 1$.

The following section will discuss the behavior of the dynamical system (4.2) at some of the equilibrium points. In this thesis the goal is to analyze the local stability of some of the equilibrium points in the invariant set $V = 0$ and the FLRW invariant set.

4.2 Local Stability

4.2.1 For P_1^* and P_2^*

P_1^* and P_2^* are lines of equilibrium points. Using the normally hyperbolic method discussed earlier (see chapter 2), we can find the stability of these equilibrium points. Moreover, after determining the Jacobian at $y = y^*$, $Q = \pm 1$, $V = 0$, we get a zero eigenvalue, and therefore the stability can be found by considering the signs of the other eigenvalues in the remaining directions. For example, when looking at P_1^* when $\epsilon = 1$, the non-zero eigenvalues are given by $\lambda_2 = -\frac{2}{3}y\sqrt{3} + \frac{4}{3}\sqrt{3}$ and $\lambda_3 = \sqrt{3} - k\sqrt{2}\sqrt{1-c^2y^2}$, and by applying the normally hyperbolic method we found that if $c < \frac{1}{2}$, $4c^2 + \frac{3}{2k^2} < 1$ and $k > \sqrt{\frac{3}{2}}$ then a part of the line P_1^* is sink if the following condition hold: $2 < y^* < \frac{1}{c}\sqrt{1-\frac{3}{2k^2}}$; otherwise, it is not stable. By implementing the same calculation we can obtain the behavior for P_1^* and P_2^* as shown in the following

table.

Table (4.3) provides the eigenvalues of the equilibrium points P_1^* and P_2^* and their stability.

Eq Pt	Eigenvalues	Sink Conditions
${}^{+}P_1^*$	$\lambda_1 = 0$ $\lambda_2 = -\frac{2}{3}y^*\sqrt{3} + \frac{4}{3}\sqrt{3}$ $\lambda_3 = \sqrt{3} - \sqrt{2}\sqrt{1 - c^2y^{*2}}k$	The only part of ${}^{+}P_1$ is a sink if $c < \frac{1}{2}$, $k > \sqrt{\frac{3}{2}}$ $4c^2 + \frac{3}{2k^2} < 1$, $2 < y^* < \frac{1}{c}\sqrt{1 - \frac{3}{2k^2}}$
${}^{-}P_1^*$	$\lambda_1 = 0$ $\lambda_2 = -\frac{2}{3}y^*\sqrt{3} + \frac{4}{3}\sqrt{3}$ $\lambda_3 = \sqrt{3} + \sqrt{2}\sqrt{1 - c^2y^{*2}}k$	No sink from λ_3
${}^{+}P_2^*$	$\lambda_1 = 0$ $\lambda_2 = -\frac{2}{3}y^*\sqrt{3} - \frac{4}{3}\sqrt{3}$ $\lambda_3 = -\sqrt{3} - \sqrt{2}\sqrt{1 - c^2y^{*2}}k$	If $c < \frac{1}{2}$ then $-2 < y^* < \frac{1}{c}$ is the only part is a sink. 2) If $c > \frac{1}{2}$ then the entire line of ${}^{+}P_2$ is a sink, $-\frac{1}{c} < y^* < \frac{1}{c}$
${}^{-}P_2^*$	$\lambda_1 = 0$ $\lambda_2 = -\frac{2}{3}y^*\sqrt{3} - \frac{4}{3}\sqrt{3}$ $\lambda_3 = -\sqrt{3} + \sqrt{2}\sqrt{1 - c^2y^{*2}}k$	1) If $c < \frac{1}{2}$, $k > \sqrt{\frac{3}{2}}$, $4c^2 + \frac{3}{2k^2} > 1$ then $-2 < y^* < -\frac{1}{c}\sqrt{1 - \frac{3}{2k^2}}$ is the only part is a sink. 2) If $c < \frac{1}{2}$, $k > \sqrt{\frac{3}{2}}$ then $\frac{1}{c}\sqrt{1 - \frac{3}{2k^2}} < y^* < \frac{1}{c}$ is the only part is a sink. 3) If $c > \frac{1}{2}$, $k > \sqrt{\frac{3}{2}}$ then $-\frac{1}{c} < y^* < -\frac{1}{c}\sqrt{1 - \frac{3}{2k^2}}$ or $\frac{1}{c}\sqrt{1 - \frac{3}{2k^2}} < y^* < \frac{1}{c}$ are the only parts that are sinks. 4) If $c < \frac{1}{2}$, $k < \sqrt{\frac{3}{2}}$ then $-2 < y^* < \frac{1}{c}$ is the only part is a sink. 5) If $c > \frac{1}{2}$, $k < \sqrt{\frac{3}{2}}$ then the entire line is sink $-\frac{1}{c} < y^* < \frac{1}{c}$

Table 4.3: The behaviour for the line fixed points P_1^* and P_2^*

4.2.2 For P_3 and P_4

When looking at the equilibrium point, P_3 (where $y = \frac{1}{c}$, $Q = 2c$, $V = 0$) for the case $\epsilon = 1$, we will never be able to calculate the Jacobian at this point because the point is non-hyperbolic. Therefore, other methods are needed to determine the stability of the 3-D system shown in (4.2). Let us instead of substituting for x restore x and substitute for y in 4- dimensional dynamical system and then rewrite the system in terms of (x,Q,V) instead of (y,Q,V), to obtain the following:

$$\begin{aligned} x' &= -2\frac{\sqrt{3}}{3}xQ + \sqrt{2}kV^2 + \frac{\sqrt{3}}{\sqrt{2}}\alpha kQV - \frac{\sqrt{3}}{3}xQ\Bigg[-2(1-x^2-V^2) - \\ &\quad 2x^2 + V^2 + 3\frac{\sqrt{2}}{2}\alpha kxV\Bigg] + \frac{\sqrt{3}}{3c}x(1-Q^2)\sqrt{1-x^2-V^2}, \\ Q' &= \frac{(1-Q^2)}{\sqrt{3}}\left[\frac{Q}{c}\sqrt{1-x^2-V^2} - 2 + 3V^2 + \frac{3\sqrt{2}}{2}\alpha kxV\right], \\ V' &= V\left[\frac{\sqrt{3}}{3c}(1-Q^2)\sqrt{1-x^2-V^2} + \sqrt{3}Q(1-V^2) + kx(-\sqrt{2} - \frac{\sqrt{6}}{2}\alpha QV)\right]. \end{aligned}$$

after determining the Jacobian at the new equilibrium point $x = 0$, $Q = 2c$, $V = 0$, we get simple eigenvalues which are , $\lambda_1 = \frac{1}{\sqrt{3}}\left[\frac{1}{c} - 4c\right]$, $\lambda_2 = \frac{\sqrt{3}}{3}\left[\frac{1}{c} - 4c\right]$ and $\lambda_3 = \left[\frac{\sqrt{3}}{3c} + 2c\frac{\sqrt{3}}{3}\right]$. From this, it can seen that λ_3 is always positive, which implies there is no sink at this point. Performing a similar calculation for ${}^{-}P_3$ the same eigenvalues and behavior are obtained as ${}^{+}P_3$. Similarly, for P_4 the same eigenvalues and behavior are obtained for $\epsilon = \pm 1$ and ${}^{\pm}P_4$ is stable (sink) if $0 < c < \frac{1}{2}$; otherwise it is unstable. Table (4.4), illustrates the eigenvalues of the equilibrium points P_3 and P_4, and their stability.

Eq Pt	λ_1,λ_2,λ_3	Sink Conditions
${}^{\pm}P_3$	$\lambda_1 = \frac{1}{\sqrt{3}}(\frac{1}{c} - 4c)$ $\lambda_2 = \frac{\sqrt{3}}{3}(\frac{1}{c} - 4c)$ $\lambda_3 = (\frac{\sqrt{3}}{3c} + 2c\frac{\sqrt{3}}{3})$	No sink (from λ_3)
${}^{\pm}P_4$	$\lambda_1 = \frac{1}{\sqrt{3}}(\frac{-1}{c} + 4c)$ $\lambda_2 = \frac{\sqrt{3}}{3}(\frac{-1}{c} + 4c)$ $\lambda_3 = (-\frac{\sqrt{3}}{3c} - 2c\frac{\sqrt{3}}{3})$	$0 < c < \frac{1}{2}$

Table 4.4: The stability of P_3 and P_4

4.2.3 For P_5 and P_6

When looking at the equilibrium point, P_5 (where $y = 0$, $Q = 1$, $V = 1$), we will never be able to calculate the Jacobian at this point because the point is non-hyperbolic. Therefore, other methods are needed to determine the stability of the 3-D system shown in (4.2). Looking at the 1 - dimensional dynamical system in the invariant set ($Q = 1$ and $y = 0$) and then looking at the 2 - dimensional invariant set $Q = \pm 1$ we able to know then the stability of the full 3 - dimensional system with knowledge of what happens in the lower dimensional systems.

First: Looking at the V' equation in full (not linearized) when $y = 0$ and $Q = 1$ will determine if V is increasing or decreasing by looking at whether V' is positive or negative (first derivative test in calculus) near to $V = 1$ but less than 1. By applying the first derivative test to the 1 - dimensional autonomous differential equation:

$$V' = V\left[\sqrt{3}(1 - V^2) + \epsilon k\sqrt{1 - V^2}\left(-\sqrt{2} - \frac{\alpha\sqrt{6}}{2}V\right)\right],$$

Observe that the point $V = 1$ is stable for some values of the parameter values α and k but there does exist some parameter values in which it is unstable. So using the derivative of the derivative (i.e., concavity arguments) we are able to find the stability conditions for this point in the y=0, Q=1 invariant set. The derivative of the right hand side in the previous equation is:

$$\sqrt{3}(1 - V^2) + k\sqrt{1 - V^2}(-\sqrt{2} - \frac{\sqrt{6}}{2}\alpha V) +$$
$$V\left[-2\sqrt{3}V - kV\frac{\left(-\sqrt{2} - \frac{\alpha\sqrt{6}}{2}V\right)}{\sqrt{1 - V^2}} - \frac{1}{2}k\sqrt{1 - V^2}\sqrt{6}\alpha\right].$$

So near $V = 1$, the term $\frac{1}{\sqrt{1-V^2}}$ dominates. The coefficient of it is $[\ -k(-\sqrt{2} - \frac{\sqrt{6}\alpha}{2})]$ which determines the sign of V'' near $V = 1$. If $V'' > 0$ for values of V near $V = 1$ but less than 1, then V' is increasing to a value of 0 at $V = 1$. This means that $V' < 0$ for values of V near $V = 1$ but less than 1, and the point $V = 1$ is unstable. Alternatively if $V'' < 0$, then the point is stable.

Second: Since we now know what happens along the V direction near V=1, we expand our analysis to the in 2 - dimensional system in the 2 - dimensional invariant sets ($Q = \pm 1$). We note that the 1 - dimensional boundary $1 - c^2y^2 - V^2 = 0$ is an invariant set within the 2 - dimensional invariant set. So when $Q = \pm 1$ we will have 2-d dynamical system as follow:

$$y' = \frac{\sqrt{3}}{3} y \left[-3V^2 Q - \epsilon \frac{3\sqrt{2}}{2} \alpha k Q V \sqrt{1 - c^2y^2 - V^2} \right], \tag{4.8a}$$

$$V' = V \Bigg[\sqrt{3} Q (1 - V^2) + \epsilon k \sqrt{1 - c^2y^2 - V^2} \left(-\sqrt{2} - \frac{\alpha\sqrt{6}}{2} QV \right) \Bigg]. \tag{4.8b}$$

Using polar coordinates for y and V as follows

$$\begin{aligned} y &= \frac{r}{c} \cos(\theta) \\ V &= r \sin(\theta) \end{aligned} \tag{4.9}$$

we can determine if the 2 - dimensional dynamical system is stable or not near the point $V = 1$, $y = 0$. After using polar coordinates the dynamical system will be for θ' and r'. By using the definition of the circle for equations (4.9) which is given by

$$c^2y^2 + V^2 = r^2, \tag{4.10}$$

and then differentiating the (4.10) and using (4.8) we will end up with r' equation as follows:

$$r' = \sqrt{3} r \sin^2(\theta) Q (1 - r^2) + rk \sin(\theta) \sqrt{1 - r^2} \left(-\sqrt{2} \sin(\theta) \right.$$

$$-\frac{\alpha\sqrt{6}}{2}r\sin^2(\theta)Q-\frac{\sqrt{6}}{2}\alpha rQ\cos^2(\theta)\Big).$$

The equilibrium point V=1, y=0 corresponds to $r=1$ and $\theta=\frac{\pi}{2}$. We can see easily that $r'=0$ when $r=1$ and that $r'>0$ for $\alpha<-\frac{2}{\sqrt{3}}$ and θ near $\frac{\pi}{2}$ by using the same analysis that we used in the 1 - dimensional invariant set. Finding θ' equation was found by using the definition $\tan\theta=\frac{V}{cy}$ and then do some calculations we will arrive to θ' when $r=1$ as follow:

$$\theta'=\sqrt{3}\sin(\theta)\cos(\theta)Q.$$

looking at θ' will determine if θ is increasing or decreasing by looking at whether θ' is positive or negative (first derivative test in calculus) near $\theta=\frac{\pi}{2}$. So when $Q=1$ in ${}^{+}P_5$ case we can see that it is a sink point in the 2 -dimensional system if $\alpha<-\frac{2}{\sqrt{3}}$. Now we can move onto the full 3 - dimensional dynamical system after we know what happens in the lower dimensional system by doing some numerical analysis for the 3-dimensional dynamical system. We see that the numerical analysis breaks down which indicates that it is unstable or something else see the following figure.

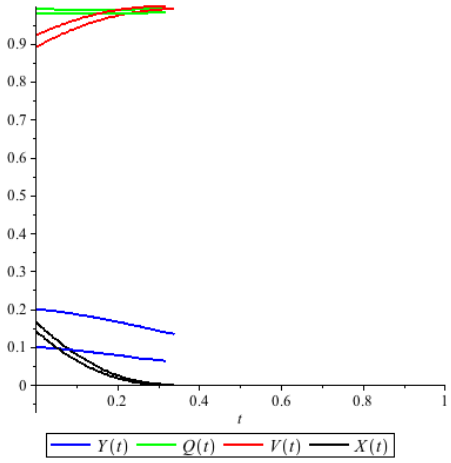

Figure 4.1: The numerical graph of the solution curves for ${}^{+}P_5$ when $\alpha=-2$, $k=1$ and $c=1$, and with this initial condition $y(0)=0.2, Q(0)=0.9$ and $V=0.9$

We now we need to look at the full 4 -dimensional dynamical system to study the stability to this point.

$$x' = -\frac{2\sqrt{3}}{3}Qx+\sqrt{2}kV^2+\frac{\sqrt{3}}{\sqrt{2}}kV\alpha Q-\frac{\sqrt{3}xQ}{3}\Big[-2c^2y^2-2x^2+V^2$$

$$
\begin{aligned}
& +\frac{3\sqrt{2}}{2}\alpha k V x\Bigg] + \frac{\sqrt{3}}{3}xy(1-Q^2), \\
Q' &= \frac{(1-Q^2)}{\sqrt{3}}\left[Qy - 2 + 3V^2 + \epsilon\frac{3\sqrt{2}}{2}\alpha k V\sqrt{1-c^2y^2-V^2}\right], \\
y' &= \frac{\sqrt{3}}{3}y\left[y - Q\left(yQ + 3V^2 + \epsilon\frac{3\sqrt{2}}{2}\alpha k V\sqrt{1-c^2y^2-V^2}\right)\right] - \frac{\sqrt{3}(1-Q^2)}{3c^2}, \\
V' &= V\Bigg[\frac{\sqrt{3}}{3}y(1-Q^2) + \sqrt{3}Q(1-V^2) \\
& \quad +\epsilon k\sqrt{1-c^2y^2-V^2}\left(-\sqrt{2} - \frac{\alpha\sqrt{6}}{2}QV\right)\Bigg].
\end{aligned}
$$

From the x definition we know that it could be positive or negative, $x = \epsilon\sqrt{1-c^2y^2-V^2}$, but we have assume that the value under the square root should be positive or zero, otherwise the root sign becomes complex. Let us study the 3 - dimensional equilibrium point $(y = 0, Q = 1, V = 1)$ which implies that $x = 0$ within this 4 - dimensional dynamical system and see what will happen to the system. Looking at the x' equation when $x = 0, y = 0, V = 1$ and $Q = 1$ will determine if x is increasing or decreasing by looking at whether x' is positive or negative we will get the following:

$$x' = \frac{\sqrt{3}}{\sqrt{2}}k(\frac{2}{\sqrt{3}} + \alpha).$$

From the 2 - dimensional dynamical system in the invariant set $(Q = 1)$ we know that ${}^{+}P_5$ is stable only if $\alpha < \frac{-2}{\sqrt{3}}$ which implies that $x' < 0$ when $x = 0$ at this ${}^{+}P_5$. That means ${}^{+}P_5$ is unstable in the 3 - dimensional dynamical system. It is the point in which trajectories pass from the positive branch (epsilon = +1) to the other (epsilon=-1). This strange behavior occurs that because we applied a global substitution for x when it clearly should not have been applied. Similarly, by doing the same method for point ${}^{-}P_5$ and ${}^{\pm}P_6$ we will find that they are unstable points.

4.2.4 For P_7 to P_{10}

The following table is included in this thesis for completeness of presentation; however, the results have not been checked [34].

Eq Pt	Existence Condition	Eigenvalues	Sink Conditions
${}^{+}P_7$	1) $\alpha > 0 \Rightarrow k < \sqrt{\frac{3}{2}}$ 2) $\alpha < 0, \quad \alpha < \frac{-2}{\sqrt{3}}$ and $k < \sqrt{\frac{3}{2}}$	$\lambda_{1,3} = -\frac{\sqrt{2}V_7 k}{2\sqrt{1-V_7^2}}\left[\sqrt{3}\alpha + 2V_7\right]$ $\lambda_2 = 2\left[\alpha k^2 V_7 + \frac{\sqrt{3}}{3}(2k^2-1)\right]$	1) If $\alpha > 0$, $\frac{1}{\sqrt{6}} < k < \sqrt{\frac{3}{2}}$ 2) If $\alpha < 0$, $\alpha < \frac{-2}{\sqrt{3}}$ $\frac{1}{\sqrt{6}} < k < \sqrt{3}$
${}^{+}P_9$	$\alpha > 0, \quad \alpha > \frac{-2}{\sqrt{3}}$ $k < \sqrt{\frac{3}{2}}$	$\lambda_{1,3} = -\frac{\sqrt{2}V_9 k}{2\sqrt{1-V_9^2}}\left[\sqrt{3}\alpha + 2V_9\right]$ $\lambda_2 = 2\left[\alpha k^2 V_9 + \frac{\sqrt{3}}{3}(2k^2-1)\right]$	No Sink
${}^{-}P_7$	$\alpha < 0$ $\alpha < \frac{-2}{\sqrt{3}}$ $k < \sqrt{\frac{3}{2}}$	$\lambda_{1,3} = \frac{\sqrt{2}V_7 k}{2\sqrt{1-V_7^2}}\left[\sqrt{3}\alpha + 2V_7\right]$ $\lambda_2 = 2\left[\alpha k^2 V_7 + \frac{\sqrt{3}}{3}(2k^2-1)\right]$	No sink
${}^{-}P_9$	$\alpha > 0$ $k < \sqrt{\frac{3}{2}}$ $\alpha < \frac{-2}{\sqrt{3}}$	$\lambda_{1,3} = \frac{\sqrt{2}V_9 k}{2\sqrt{1-V_9^2}}\left[-\sqrt{3}\alpha + 2V_9\right]$ $\lambda_2 = 2\left[\alpha k^2 V_9 - \frac{\sqrt{3}}{3}(2k^2-1)\right]$	$\alpha > 0$ $\frac{1}{\sqrt{6}} < k < \sqrt{\frac{3}{2}}$ $\frac{3}{4} < \frac{1}{\alpha^2} < \frac{k^2(6k^2-1)}{2(1-2k^2)^2}$ $\alpha^2 < \frac{4}{3} - \frac{2}{k^2}$

Table 4.5: The stability of P_7 and P_9

4.3 Table of Sinks

Table (4.6) illustrates, for different parameter values, all of the sinks with either $V = 0$, or in which $y = 0$ and $Q = \pm 1$. For lines of equilibrium points, the interval that is a sink is given. The following table shows the sinks when $c < \frac{1}{2}$ for different values of k and α.

,

$c, k > 0$	$k : 0 \longrightarrow \frac{1}{\sqrt{6}}$	$k : \frac{1}{\sqrt{6}} \longrightarrow \sqrt{\frac{3}{2}}$	$k > \sqrt{\frac{3}{2}}$	sink conditions
$\alpha > 0$			${}^{+}P_1$	$2 < y^* < \frac{1}{c}\sqrt{1 - \frac{3}{2k^2}}$, $4c^2 + \frac{3}{2k^2} < 1$
	${}^{+}P_2$	${}^{+}P_2$	${}^{+}P_2$	$-2 < y^* < \frac{1}{c}$
	${}^{-}P_2$	${}^{-}P_2$		$-2 < y^* < \frac{1}{c}$
			${}^{-}P_2$	1) $4c^2 + \frac{3}{2k^2} > 1$,$-2 < y^* < -\frac{1}{c}\sqrt{1 - \frac{3}{2k^2}}$
				2) $\frac{1}{c}\sqrt{1 - \frac{3}{2k^2}} < y^* < \frac{1}{c}$
	${}^{\pm}P_4$	${}^{\pm}P_4$	${}^{\pm}P_4$	
$\frac{-2}{\sqrt{3}} < \alpha < 0$			${}^{+}P_1$	$2 < y^* < \frac{1}{c}\sqrt{1 - \frac{3}{2k^2}}$, $4c^2 + \frac{3}{2k^2} < 1$
	${}^{+}P_2$	${}^{+}P_2$	${}^{+}P_2$	$-2 < y* < \frac{1}{c}$
	${}^{-}P_2$	${}^{-}P_2$		$-2 < y^* < \frac{1}{c}$
			${}^{-}P_2$	1) $4c^2 + \frac{3}{2k^2} > 1$,$-2 < y^* < -\frac{1}{c}\sqrt{1 - \frac{3}{2k^2}}$
				2) $\frac{1}{c}\sqrt{1 - \frac{3}{2k^2}} < y^* < \frac{1}{c}$
	${}^{\pm}P_4$	${}^{\pm}P_4$	${}^{\pm}P_4$	
$\alpha < \frac{-2}{\sqrt{3}}$			${}^{+}P_1$	$2 < y^* < \frac{1}{c}\sqrt{1 - \frac{3}{2k^2}}$, $4c^2 + \frac{3}{2k^2} < 1$
	${}^{+}P_2$	${}^{+}P_2$	${}^{+}P_2$	$-2 < y^* < \frac{1}{c}$
	${}^{-}P_2$	${}^{-}P_2$		$-2 < y^* < \frac{1}{c}$,
			${}^{-}P_2$	1) $4c^2 + \frac{3}{2k^2} > 1$,$-2 < y^* < -\frac{1}{c}\sqrt{1 - \frac{3}{2k^2}}$
				2) $\frac{1}{c}\sqrt{1 - \frac{3}{2k^2}} < y^* < \frac{1}{c}$
	${}^{\pm}P_4$	${}^{\pm}P_4$	${}^{\pm}P_4$	

Table 4.6: The table of sinks conditions when $c < \frac{1}{2}$ for different values of k and α

Table (4.7) illustrates for different parameter values all of the sinks with either $V = 0$, or in which $y = 0$ and $Q = \pm 1$. For lines of equilibrium, the interval that is a sink is given. The following table shows the sinks when $c > \frac{1}{2}$ for different values of k and α.

,

$c, k > 0$	$k : 0 \longrightarrow \frac{1}{\sqrt{6}}$	$k : \frac{1}{\sqrt{6}} \longrightarrow \sqrt{\frac{3}{2}}$	$k > \sqrt{\frac{3}{2}}$	sink conditions
$\alpha > 0$	${}^{+}P_2$	${}^{+}P_2$	${}^{+}P_2$	$-\frac{1}{c} < y^* < \frac{1}{c}$
	${}^{-}P_2$	${}^{-}P_2$		$-\frac{1}{c} < y^* < \frac{1}{c}$
			${}^{-}P_2$	$\frac{1}{c}\sqrt{1-\frac{3}{2k^2}} < y^* < \frac{1}{c}$
				or $-\frac{1}{c} < y^* < -\frac{1}{c}\sqrt{1-\frac{3}{2k^2}}$
$\frac{-2}{\sqrt{3}} < \alpha < 0$	${}^{+}P_2$	${}^{+}P_2$	${}^{+}P_2$	$-\frac{1}{c} < y* < \frac{1}{c}$
	${}^{-}P_2$	${}^{-}P_2$		$-\frac{1}{c} < y^* < \frac{1}{c}$
			${}^{-}P_2$	$\frac{1}{c}\sqrt{1-\frac{3}{2k^2}} < y^* < \frac{1}{c}$
				or $-\frac{1}{c} < y^* < -\frac{1}{c}\sqrt{1-\frac{3}{2k^2}}$
$\alpha < \frac{-2}{\sqrt{3}}$	${}^{+}P_2$	${}^{+}P_2$	${}^{+}P_2$	$-\frac{1}{c} < y^* < \frac{1}{c}$
	${}^{-}P_2$	${}^{-}P_2$		$-\frac{1}{c} < y^* < \frac{1}{c}$,
			${}^{-}P_2$	$\frac{1}{c}\sqrt{1-\frac{3}{2k^2}} < y^* < \frac{1}{c}$
				or $-\frac{1}{c} < y^* < -\frac{1}{c}\sqrt{1-\frac{3}{2k^2}}$

Table 4.7: The table of sinks conditions when $c > \frac{1}{2}$ for different values of k and α

4.4 Alternative Table of Sink

Table (4.8) and (4.9) show that the stability of the equilibrium points do not depend on the value of α at all depend in c, k only.
Table (4.9) shows the sink and their dependencies on the parameter k with $c < \frac{1}{2}$ showing the different intervals for the sink.

$-\infty < \alpha < \infty$	$k < \sqrt{\frac{3}{2}}$	$k > \sqrt{\frac{3}{2}}$	sink conditions
$c < \frac{1}{2}$		${}^{+}P_1$	$4c^2 + \frac{3}{2k^2} < 1$, $2 < y^* < \frac{1}{c}\sqrt{1 - \frac{3}{2k^2}}$,
	${}^{+}P_2$	${}^{+}P_2$	$-2 < y^* < \frac{1}{c}$
		${}^{-}P_2$	1) $4c^2 + \frac{3}{2k^2} > 1$, $-2 < y^* < -\frac{1}{c}\sqrt{1 - \frac{3}{2k^2}}$
			2) $\frac{1}{c}\sqrt{1 - \frac{3}{2k^2}} < y^* < \frac{1}{c}$
	${}^{-}P_2$		$-2 < y^* < \frac{1}{c}$
	${}^{\pm}P_4$	${}^{\pm}P_4$	

Table 4.8: The table of sinks when $c < \frac{1}{2}$ for different values of k

Table (4.9) shows the sink and their dependencies on the parameter k with $c > \frac{1}{2}$ showing the different intervals for the sink.

$-\infty < \alpha < \infty$	$k < \sqrt{\frac{3}{2}}$	$k > \sqrt{\frac{3}{2}}$	sink conditions
$c > \frac{1}{2}$	${}^{+}P_2$	${}^{+}P_2$	-$\frac{1}{c} < y^* < \frac{1}{c}$
	${}^{-}P_2$		$-\frac{1}{c} < y^* < \frac{1}{c}$
		${}^{-}P_2$	$-\frac{1}{c} < y^* < -\frac{1}{c}\sqrt{1 - \frac{3}{2k^2}}$
			or $\frac{1}{c}\sqrt{1 - \frac{3}{2k^2}} < y^* < \frac{1}{c}$

Table 4.9: The table of sinks when $c > \frac{1}{2}$ for different values of k

4.5 Numerical Analysis

This section confirms the existence of all of the sinks numerically by using Maple software.

Figures for ${}^{+}P_1$:

Figure (4.2) illustrates model (4.2) near ${}^{+}P_1$ when $c < \frac{1}{2}$,$\alpha < -\frac{2}{\sqrt{3}}$, and $k > \sqrt{\frac{3}{2}}$.

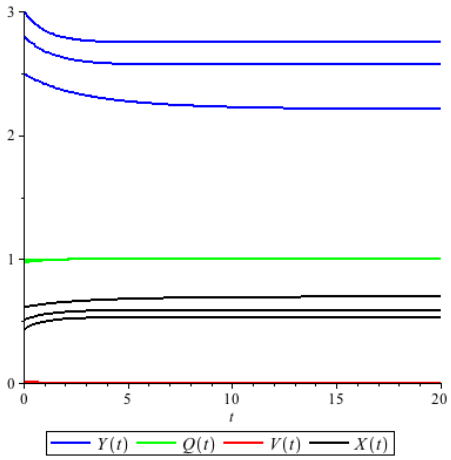

Figure 4.2: The numerical graph of the solution curves for ${}^{+}P_1$ when $\alpha = -2$, $k = 2$ and $c = \frac{1}{4}$, but with different initial conditions.

It can be seen from figure (4.2), for the values $\alpha < -\frac{2}{\sqrt{3}}$, $c < \frac{1}{2}$ and $k > \sqrt{\frac{3}{2}}$ that, ${}^{+}P_1$ is a sink because the expected outcome is that V goes to zero, Q goes to one and y goes to a point between 2 and $\frac{1}{c}\sqrt{1 - \frac{3}{2k^2}}$. Parameter values for this numerical analysis are chosen to be: $\alpha = -2$, $c = \frac{1}{4}$, $k = 2$. Initial Values are $y(0) = 2.5, Q(0) = 0.99$, $V(0) = 0.001$, $y(0) = 2.8, Q(0) = 0.98$, $V(0) = 0.003$, $y(0) = 3, Q(0) = 0.97$, $V(0) = 0.002$.

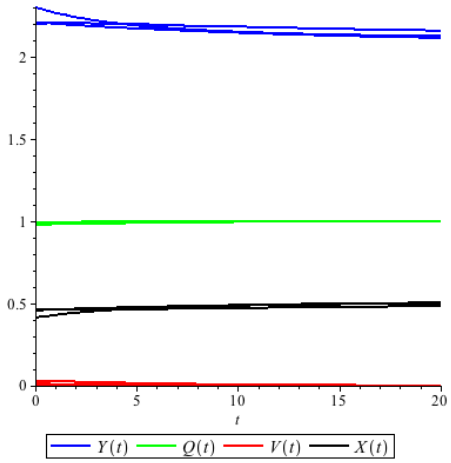

Figure 4.3: The numerical graph of the solution curves for ${}^{+}P_1$ when $\alpha = -1$, $k = 2$ and $c = \frac{1}{3}$, but with different initial conditions.

It can be seen from figure (4.3), for the values $\alpha > \frac{-2}{\sqrt{3}}$, $c < \frac{1}{2}$ and $k > \sqrt{\frac{3}{2}}$ that, ${}^{+}P_1$ is a sink because the expected outcome is that V goes to zero, Q goes to one and y goes to point between 2 and $\frac{1}{c}\sqrt{1 - \frac{3}{2k^2}}$. Parameter values for this numerical analysis are chosen to be: $\alpha = -1$, $c = \frac{1}{3}$, $k = 2$. Initial Values are $y(0) = 2.3, Q(0) = 0.99$, $V(0) = 0.001$, $y(0) = 2.2, Q(0) = 0.979$, $V(0) = 0.03$, $y(0) = 2.21, Q(0) = 0.99$, $V(0) = 0.01$.

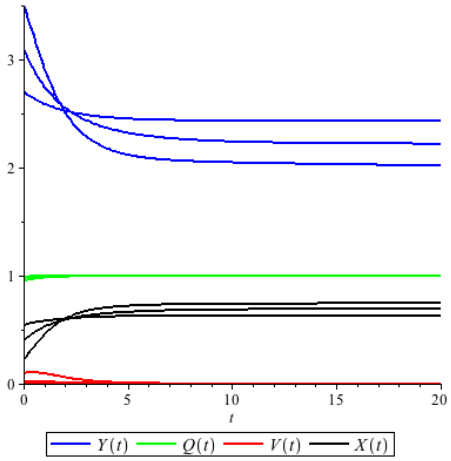

Figure 4.4: The numerical graph of the solution curves for ${}^{+}P_1$ when $\alpha = 1$, $k = 2$ and $c = \frac{1}{4}$, but with different initial conditions.

As can be seen from figure (4.4), for the values $\alpha > 0$, $c < \frac{1}{2}$ and $k > \sqrt{\frac{3}{2}}$ we have that, ${}^{+}P_1$ is a sink because the expected outcome is that V goes to zero, Q goes to one and y goes to point between 2 and $\frac{1}{c}\sqrt{1 - \frac{3}{2k^2}}$. Parameter values for this numerical analysis are chosen to be: $\alpha = 1$, $c = \frac{1}{4}$, $k = 2$. Initial Values are $y(0) = 2.7, Q(0) = 0.99$, $V(0) = 0.01$, $y(0) = 3.1, Q(0) = 0.95$, $V(0) = 0.02$, $y(0) = 3.5, Q(0) = 0.98$, $V(0) = 0.1$.

Figures for $^{+}P_2$:

Figure (4.5) plots the model (4.2) for $^{+}P_2$ on the interval $c < \frac{1}{2}$ with varying k values.

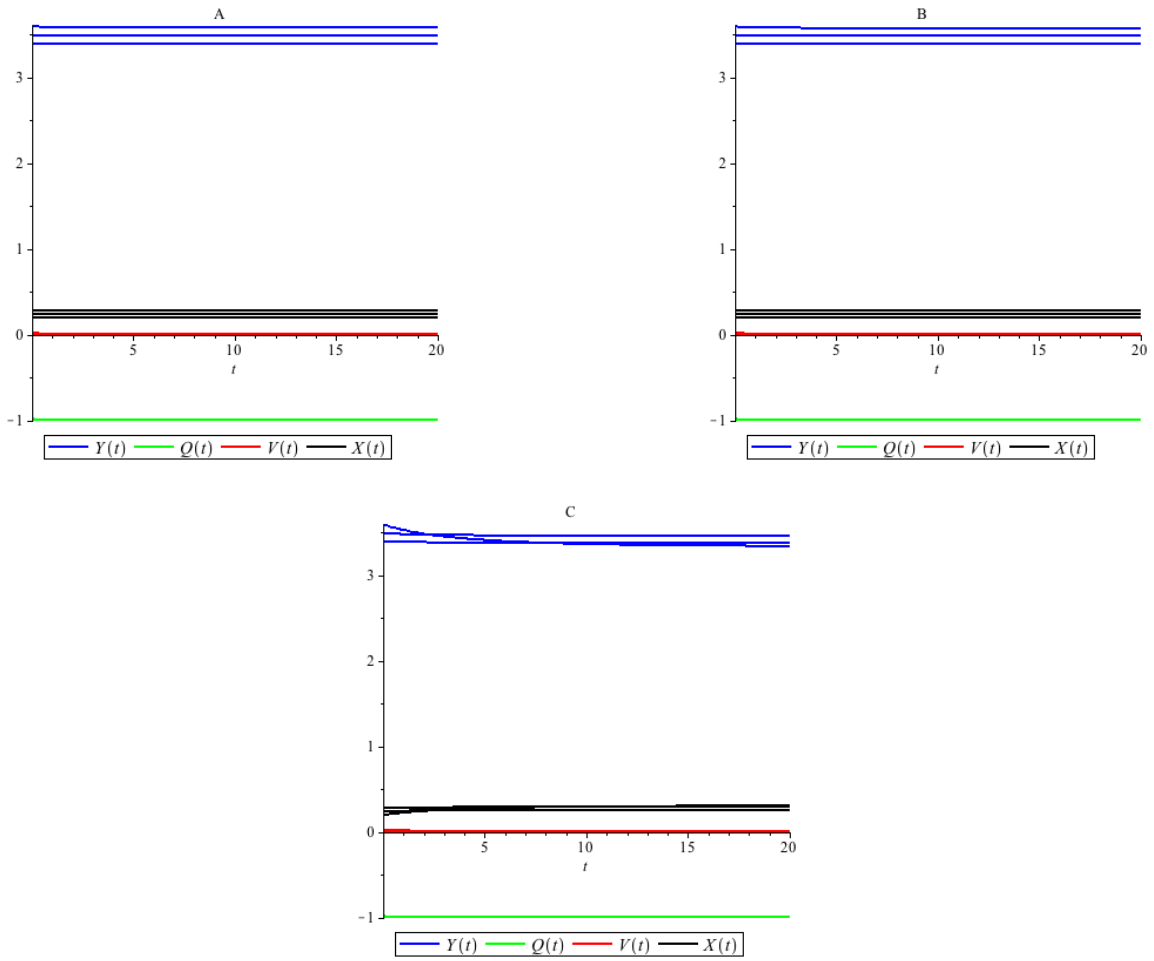

Figure 4.5: The numerical graph of the solution curves for $^{+}P_2$ when $\alpha = -1$, $c = \frac{1}{4}$ and $k = 0.1$ in figure A, $k = 0.5$ in figure B $k = 2$ in figure C, but with different initial conditions

Figure (4.5), illustrates the models with the condition of $c < \frac{1}{2}$ and varying values of k. Graphs A, B, and C indicate k values of $0 < k < \frac{1}{\sqrt{6}}$, $\frac{1}{\sqrt{6}} < k < \sqrt{\frac{3}{2}}$, and $k > \sqrt{\frac{3}{2}}$, respectively. The following parameters for this numerical analysis are chosen to be: $c = \frac{1}{4}$, and $\alpha = -1$ and the initial conditions of $y(0) = -0.89, Q(0) = -0.99$, and $V(0) = 0.001$, $y(0) = -0.99, Q(0) = -0.98$, and $V(0) = 0.02$ $y(0) = -0.98, Q(0) = -0.99$, and $V(0) = 0.03$ were selected. The k values chosen for graphs A, B and C were 0.1, 0.5 and 2, respectively. It can be seen from the graphs that, $^{+}P_2$ is a sink because the expected outcome is that V goes to zero, Q goes to negative one and y

goes to point greater than -2 and less than $\frac{1}{c}$

Figure (4.6) plots the model (4.2) for ${}^{+}P_2$ on the interval $c > \frac{1}{c}$ with varying k values.

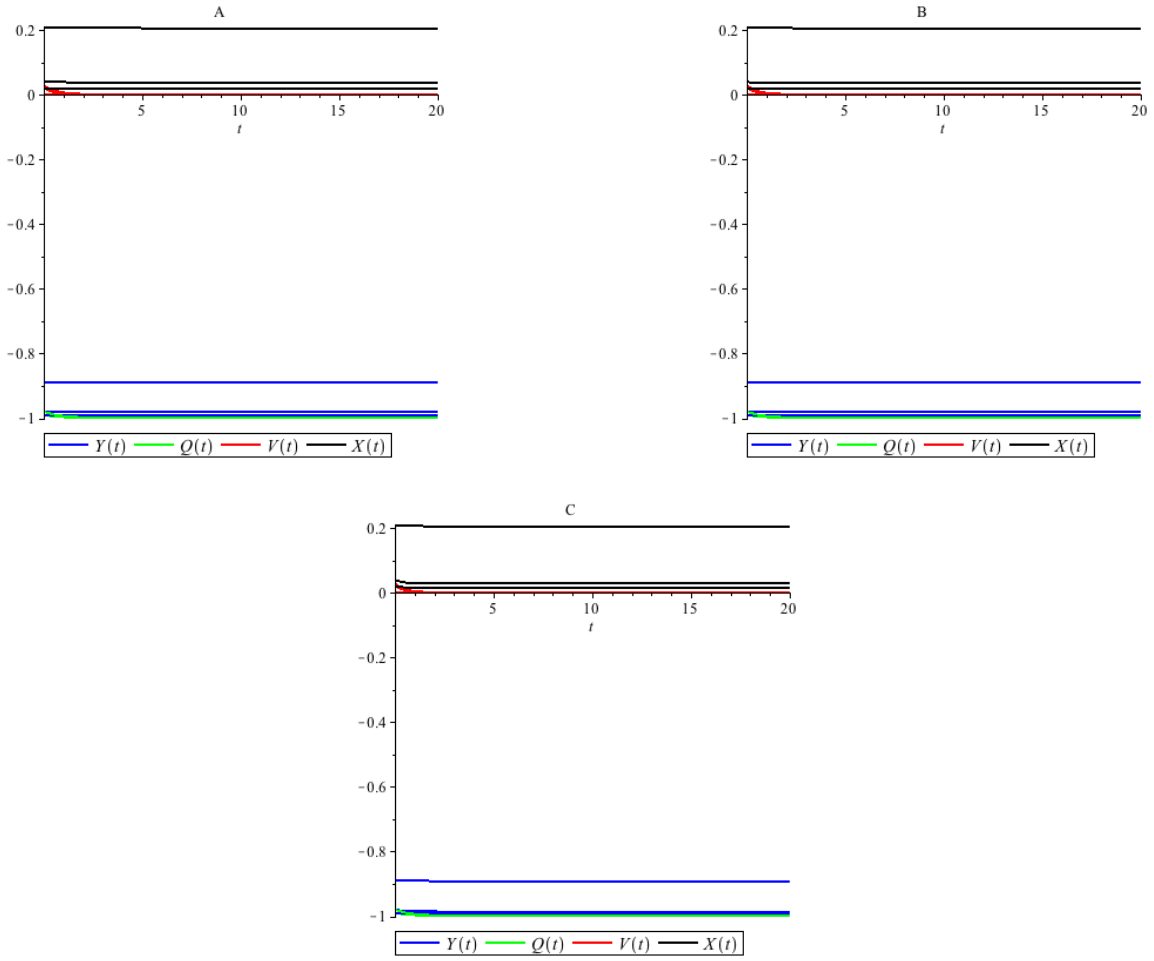

Figure 4.6: The numerical graph of the solution curves for ${}^{+}P_2$ when $\alpha = 1$, $c = 1$ and $k = 0.1$ in figure A, $k = 0.5$ in figure B $k = 2$ in figure C, but with different initial conditions.

Figure (4.6), illustrates the models with the condition of $c > \frac{1}{2}$ and varying values of k. Graphs A, B, and C indicate k values of $0 < k < \frac{1}{\sqrt{6}}$, $\frac{1}{\sqrt{6}} < k < \sqrt{\frac{3}{2}}$, and $k > \sqrt{\frac{3}{2}}$, respectively. The following parameters for this numerical analysis are chosen to be: $c = 1$, and $\alpha = 1$ and the initial conditions of $y(0) = -0.89, Q(0) = -0.99$, and $V(0) = 0.001$, $y(0) = -0.99, Q(0) = -0.98$, and $V(0) = 0.02$ $y(0) = -0.98, Q(0) = -0.99$, and $V(0) = 0.03$ were selected. The k values chosen for graphs A, B and C were 0.1, 0.5

and 2, respectively. It can be seen from the graphs that ${}^{-}P_2$ is a sink because the expected outcome is that V goes to zero, Q goes to negative one and y goes to point grater than -2 between $-\frac{1}{c} < y^* < \frac{1}{c}$.

Figures for $^{-}P_2$:

Figure (4.7) indicates the model (4.2) for $^{-}P_2$ on the interval $c < \frac{1}{2}$ and with varying k values.

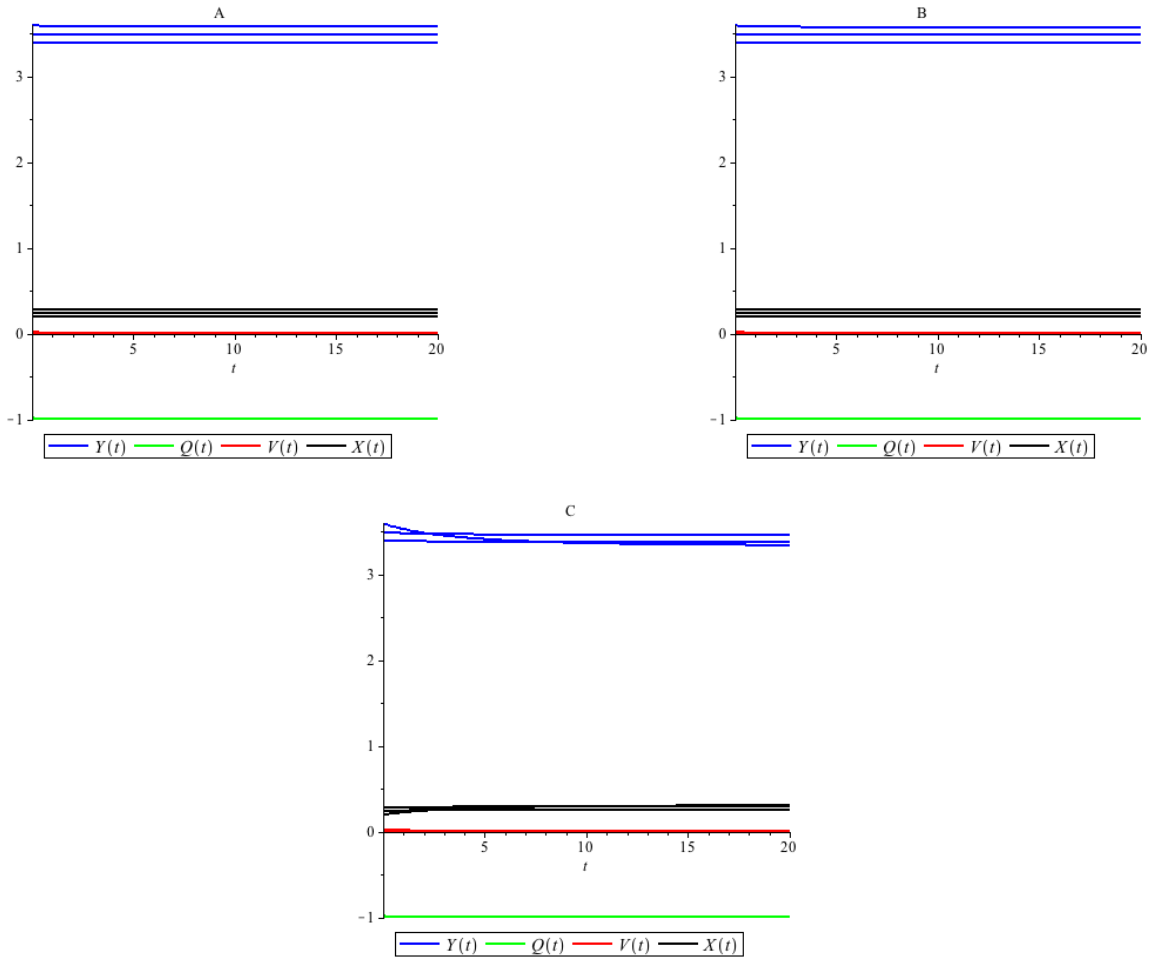

Figure 4.7: The numerical graph of the solution curves for $^{-}P_2$ when $\alpha = 1$, $c = \frac{1}{4}$ and $k = 0.1$ in figure A, $k = 0.5$ in figure B $k = 2$ in figure C, but with different initial conditions.

Figure (4.7), illustrates the models with the condition of $c < \frac{1}{2}$ and varying values of k. Graphs A, B, and C indicate k values of $0 < k < \frac{1}{\sqrt{6}}$, $\frac{1}{\sqrt{6}} < k < \sqrt{\frac{3}{2}}$, and $k > \sqrt{\frac{3}{2}}$, respectively. The following parameters for this numerical analysis are chosen to be: $c = \frac{1}{4}$, and $\alpha = 1$ and the initial conditions of $y(0) = 3.4, Q(0) = -0.99$, and $V(0) = 0.001$, $y(0) = 3.5, Q(0) = -0.98$, and $V(0) = 0.02$ $y(0) = 3.6, Q(0) = -0.98$, and $V(0) = 0.1$ were selected. The k values chosen for graphs A, B and C were 0.1, 0.5 and 2, respectively. It can be seen from the graphs that $^{-}P_2$ is a sink because the

expected outcome is that V goes to zero, Q goes to negative one and y goes to point between $\frac{1}{c}\sqrt{1-\frac{3}{2k^2}} < y^* < \frac{1}{c}$.

Figure (4.8) indicates the model (4.2) for ${}^{-}P_2$ on the interval $c > \frac{1}{c}$ and with varying k values.

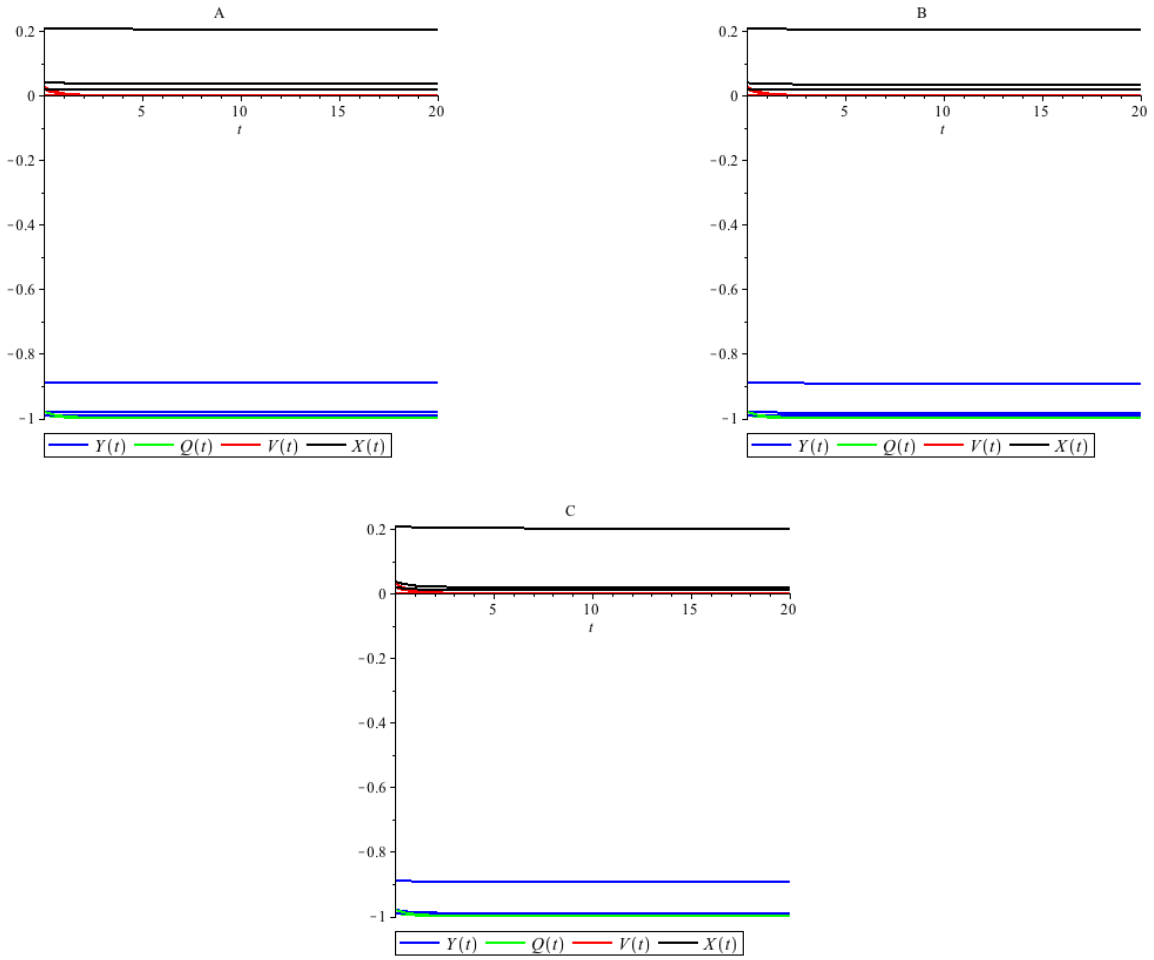

Figure 4.8: The numerical graph of the solution curves for ${}^{-}P_2$ when $\alpha = -1$, $c = 1$ and $k = 0.1$ in figure A, $k = 0.5$ in figure B $k = 2$ in figure C, but with different initial conditions.

Figure (4.8), illustrates the models with the condition of $c > \frac{1}{2}$ and varying values of k. Graphs A, B, and C indicate k values of $0 < k < \frac{1}{\sqrt{6}}$, $\frac{1}{\sqrt{6}} < k < \sqrt{\frac{3}{2}}$, and $k > \sqrt{\frac{3}{2}}$, respectively. The following parameters for this numerical analysis are chosen to be: $c = 1$, and $\alpha = -1$ and the initial conditions of $y(0) = -0.89, Q(0) = -0.99$, and $V(0) = 0.001$, $y(0) = -0.99, Q(0) = -0.98$, and $V(0) = 0.02$ $y(0) = -0.98, Q(0) =$

-0.99, and $V(0) = 0.03$ were selected. The k values chosen for graphs A, B and C were 0.1, 0.5 and 2, respectively. It can be seen from the graphs that ${}^{-}P_2$ is a sink because the expected outcome is that V goes to zero, Q goes to negative one and y goes to point between $\frac{1}{c}\sqrt{1-\frac{3}{2k^2}} < y^* < \frac{1}{c}$.

Figures for $^{+}P_4$:

Figure (4.9) plots the model (4.2) for $^{+}P_4$ on the interval $c < \frac{1}{2}$, $\alpha < -\frac{2}{\sqrt{3}}$ with varying k values.

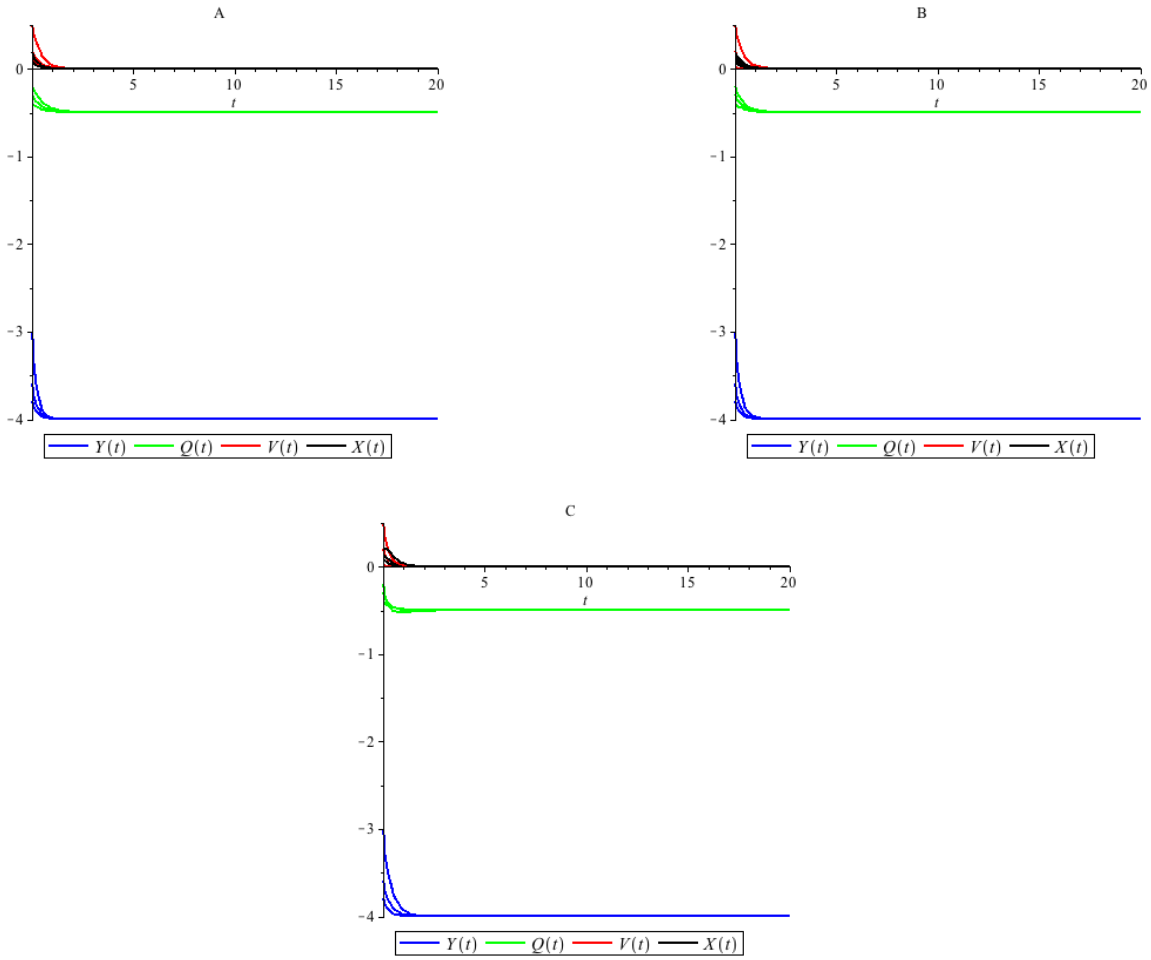

Figure 4.9: The numerical graph of the solution curves for $^{+}P_4$ when $\alpha = -2$, $c = \frac{1}{4}$ and $k = 0.1$ in figure A, $k = 0.5$ in figure B $k = 2$ in figure C, but with different initial conditions.

Figures (4.9) illustrates the models with the condition of $c < \frac{1}{2}$, $\alpha < -\frac{2}{\sqrt{3}}$ and varying values of k. Graphs A, B, and C indicate k values of $0 < k < \frac{1}{\sqrt{6}}$, $\frac{1}{\sqrt{6}} < k < \sqrt{\frac{3}{2}}$, and $k > \sqrt{\frac{3}{2}}$, respectively. The following parameters for this numerical analysis are chosen to be: $c = \frac{1}{4}$, $\alpha = -2$ and the initial conditions of $y(0) = -3.8, Q(0) = -0.4$, $V(0) = 0.1$, $y(0) = -3.6, Q(0) = -0.3$, $V(0) = 0.2$, and $y(0) = -3, Q(0) = -0.2$, $V(0) = 0.5$, were selected. The k values chosen for graphs A, B and C were 0.1, 0.5 and 2, respectively. It can be seen from the graphs that $^{+}P_4$ is a sink because the

expected outcome is that V goes to zero, Q goes to $-\frac{1}{2}$ and y goes to -4.

Figure (4.10) plots the model (4.2) for ${}^{+}P_4$ on the interval $c < \frac{1}{2,}\ \alpha > -\frac{2}{\sqrt{3}}$ with varying k values.

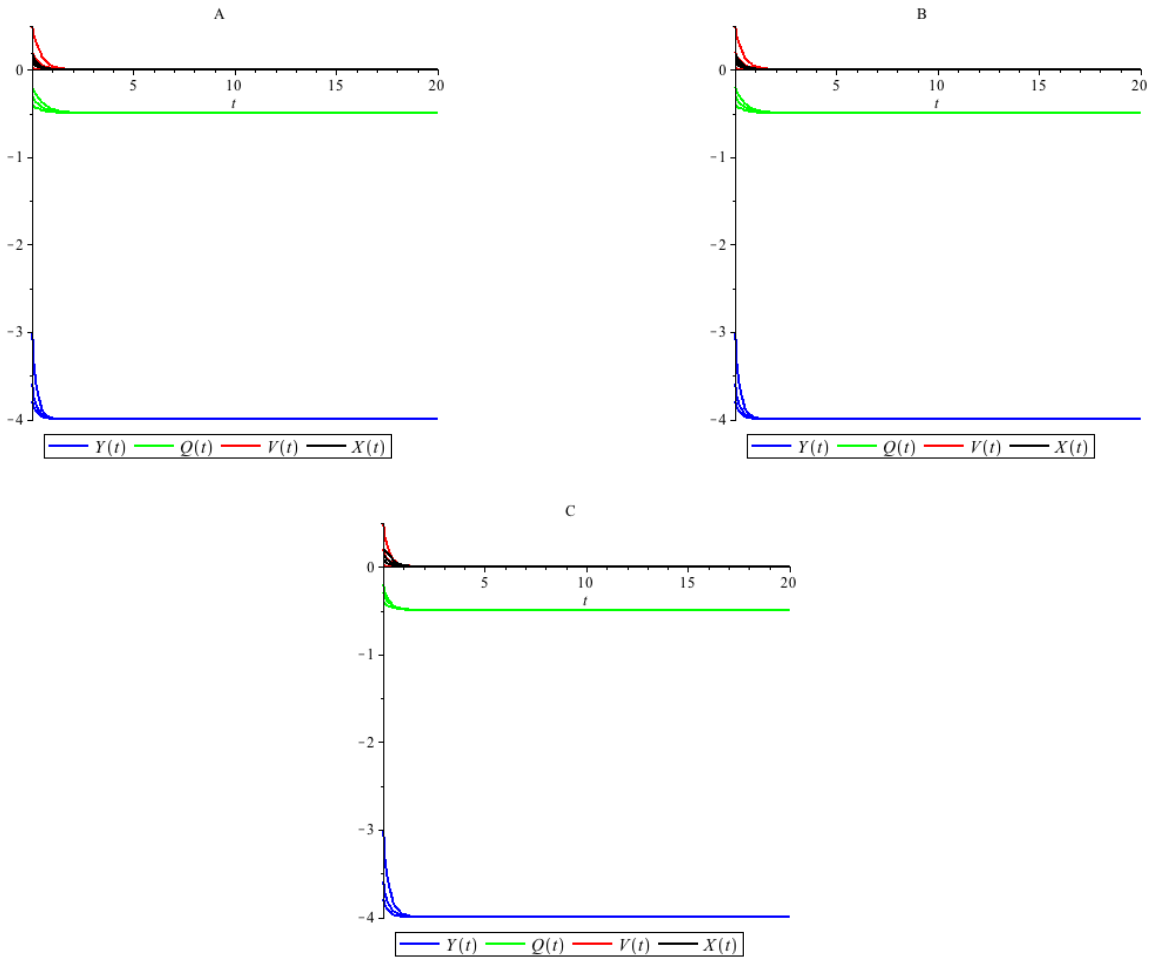

Figure 4.10: The numerical graph of the solution curves for ${}^{+}P_4$ when $\alpha = -1$, $c = \frac{1}{4}$ and $k = 0.1$ in figure A, $k = 0.5$ in figure B $k = 2$ in figure C, but with different initial conditions.

Figures (4.10) illustrates the models with the condition of $c < \frac{1}{2,}\ \alpha > -\frac{2}{\sqrt{3}}$ and varying values of k. Graphs A, B, and C indicate k values of $0 < k < \frac{1}{\sqrt{6}}$, $\frac{1}{\sqrt{6}} < k < \sqrt{\frac{3}{2}}$, and $k > \sqrt{\frac{3}{2}}$, respectively. In the figures, the same parameters and initial conditions were selected as in figures (4.9), except here $\alpha = -1$, so we have that ${}^{+}P_4$ is a sink because the expected outcome is that V goes to zero, Q goes to $-\frac{1}{2}$ and y goes to -4.

Figure (4.11) plots the model (4.2) for ${}^{+}P_4$ on the interval $c < \frac{1}{2}$, $\alpha > 0$ with varying k values.

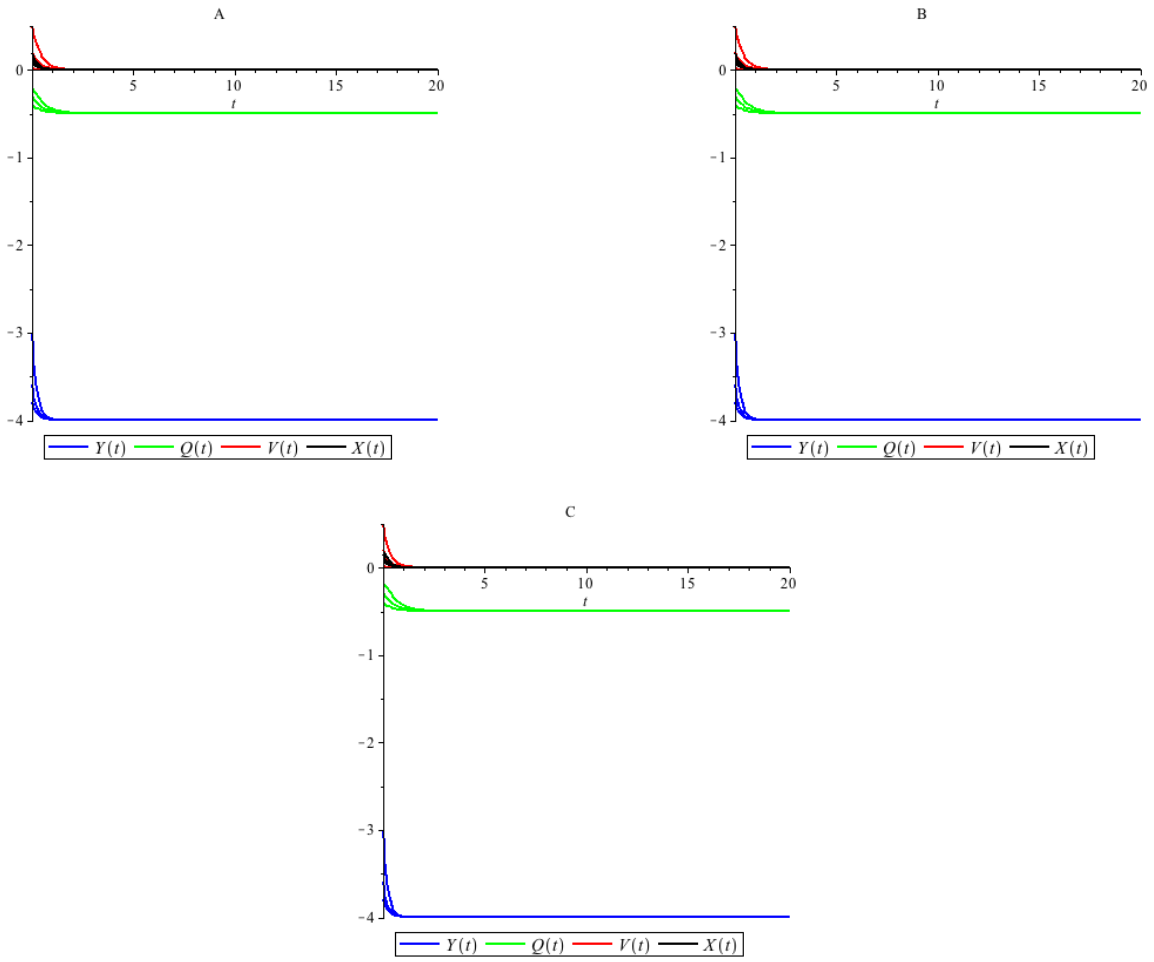

Figure 4.11: The numerical graph of the solution curves for ${}^{+}P_4$ when $\alpha = 1$, $c = \frac{1}{4}$ and $k = 0.1$ in figure A, $k = 0.5$ in figure B $k = 2$ in figure C, but with different initial conditions.

Figures (4.11) illustrates the models with the condition of $c < \frac{1}{2}$, $\alpha > 0$ and varying values of k. Graphs A, B, and C indicate k values of $0 < k < \frac{1}{\sqrt{6}}$, $\frac{1}{\sqrt{6}} < k < \sqrt{\frac{3}{2}}$, and $k > \sqrt{\frac{3}{2}}$, respectively. In the figures, the same parameters and initial conditions were selected as in figures (4.9), except here $\alpha = 1$, so we have that ${}^{+}P_4$ is sink because the expected outcome is that V goes to zero, Q goes to $-\frac{1}{2}$ and y goes to -4.

Figures for $^{-}P_4$:

Figure (4.12) plots the model (4.2) for $^{-}P_4$ on the interval $c < \frac{1}{2}$, $\alpha < -\frac{2}{\sqrt{3}}$ with varying k values.

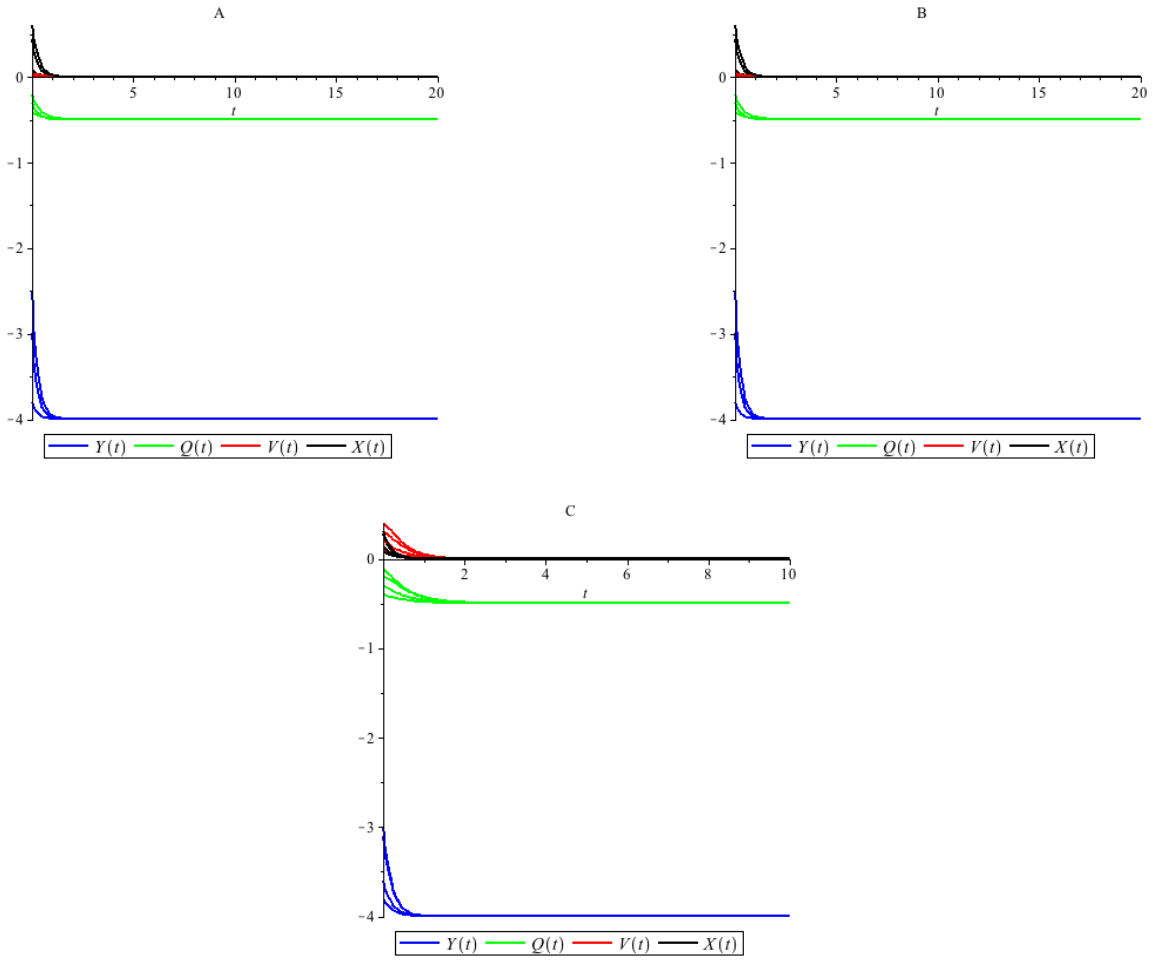

Figure 4.12: The numerical graph of the solution curves for $^{-}P_4$ when $\alpha = -2$, $c = \frac{1}{4}$ and $k = 0.1$ in figure A, $k = 0.5$ in figure B $k = 2$ in figure C, but with different initial conditions.

Figures (4.12) illustrates the models with the condition of $c < \frac{1}{2}$, $\alpha < -\frac{2}{\sqrt{3}}$ and varying values of k. Graphs A, B, and C indicate k values of $0 < k < \frac{1}{\sqrt{6}}$, $\frac{1}{\sqrt{6}} < k < \sqrt{\frac{3}{2}}$, and $k > \sqrt{\frac{3}{2}}$, respectively. The following parameters for this numerical analysis are chosen to be: $c = \frac{1}{4}$, $\alpha = -2$ and the initial conditions of $y(0) = -3.8, Q(0) = -0.4$, $V(0) = 0.01$, $y(0) = -3.6, Q(0) = -0.3$, $V(0) = 0.02$, and $y(0) = -2.5, Q(0) = -0.3$, $V(0) = 0.04$, were selected. The k values chosen for graphs A, B and C were 0.1, 0.5 and 2, respectively. It can be seen from the graphs that $^{-}P_4$ is a sink because the

expected outcome is that V goes to zero, Q goes to $-\frac{1}{2}$ and y goes to -4.

Figure (4.13) plots the model (4.2) for ${}^{-}P_4$ on the interval $c < \frac{1}{2}$ $\alpha > -\frac{2}{\sqrt{3}}$ with varying k values.

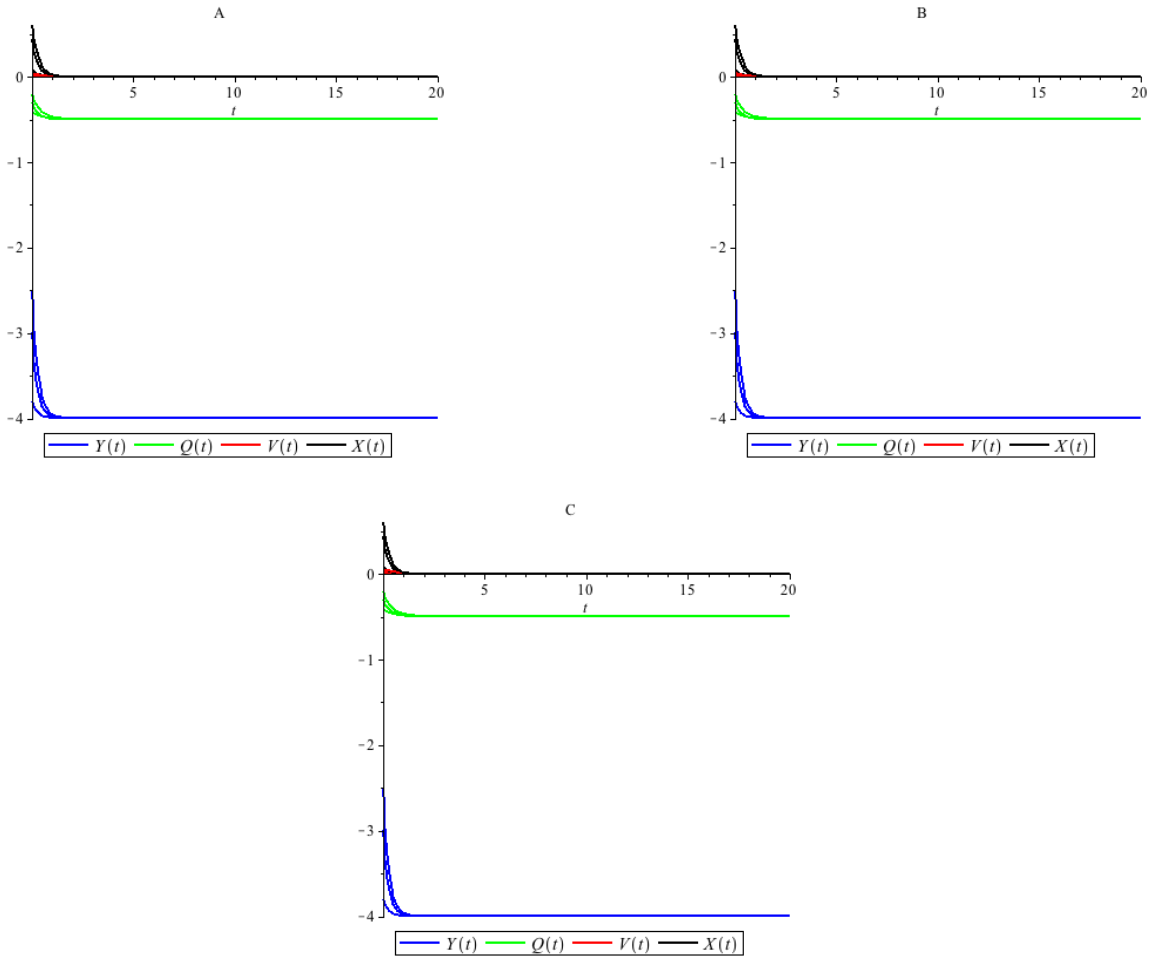

Figure 4.13: The numerical graph of the solution curves for ${}^{-}P_4$ when $\alpha = -1$, $c = \frac{1}{4}$ and $k = 0.1$ in figure A, $k = 0.5$ in figure B $k = 2$ in figure C, but with different initial conditions.

Figures (4.13), illustrates the models with the condition of $c < \frac{1}{2}$, $\alpha > -\frac{2}{\sqrt{3}}$ and varying values of k. Graphs A, B, and C indicate k values of $0 < k < \frac{1}{\sqrt{6}}$, $\frac{1}{\sqrt{6}} < k < \sqrt{\frac{3}{2}}$, and $k > \sqrt{\frac{3}{2}}$, respectively. The models take into consideration the sink conditions outlined in table (4.6). In the figures, the same parameters and initial conditions were selected as in figures (4.13) except here $\alpha = -1$, so we have that ${}^{-}P_4$ is sink because the expected outcome is that V goes to zero, Q goes to $-\frac{1}{2}$ and y goes to -4.

Figure (4.14) plots the model (4.2) for ${}^{-}P_4$ on the interval $c < \frac{1}{2}$, $\alpha > 0$ with varying k values.

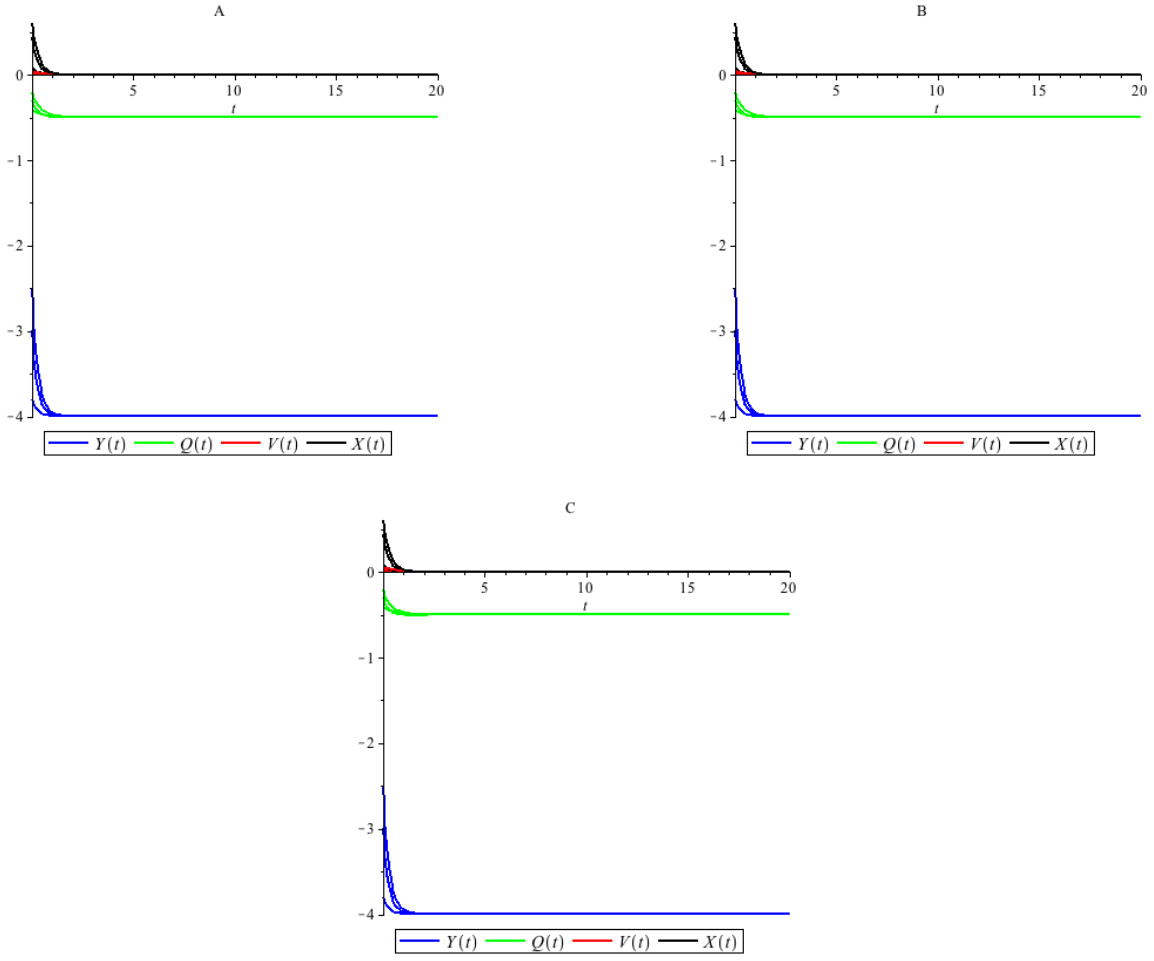

Figure 4.14: The numerical graph of the solution curves for ${}^{-}P_4$ when $\alpha = 1$, $c = \frac{1}{4}$ and $k = 0.1$ in figure A, $k = 0.5$ in figure B $k = 2$ in figure C, but with different initial conditions.

Figures (4.14), illustrates the models with the condition of $c < \frac{1}{2}$, $\alpha > 0$ and varying values of k. Graphs A, B, and C indicate k values of $0 < k < \frac{1}{\sqrt{6}}$, $\frac{1}{\sqrt{6}} < k < \sqrt{\frac{3}{2}}$, and $k > \sqrt{\frac{3}{2}}$, respectively. The models take into consideration the sink conditions outlined in table (4.6). In the figures, the same parameters and initial conditions were selected as in figures (4.13), except here $\alpha = 1$, so we have that ${}^{-}P_4$ is sink because the expected outcome is that V goes to zero, Q goes to $-\frac{1}{2}$ and y goes to -4.

Figures for $^{+}P_5$:

Figure (4.15) shows the direction field plot for the 2 - dimensional dynamical system (4.8) in which $\alpha < -\frac{2}{\sqrt{3}}$ and $k > 0$ in the 2 - dimensional set, $Q = 1$. We observe that the point $^{+}P_5$ is stable in the 2-dimensional invariant set for all values of k provided $\alpha < -\frac{2}{\sqrt{3}}$.

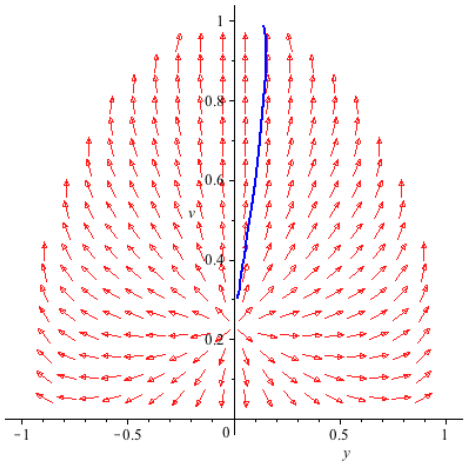

Figure 4.15: The numerical graph of the solution curves for $^{+}P_5$ when $\alpha = -2$, $k = 2$ and $c = 1$.

Graph (4.15) indicates the direction field plot for the the 2 - dimensional dynamical system (4.8) in which $c = 1$,$k = 2$ and $\alpha = -2$. The initial condition $y(0) = 0.02$ and $V = 0.3$ were selected. It can be seen from the graphs that $^{+}P_5$ is a sink in the 2 - dimensional set, Q=1 when $\alpha < -\frac{2}{\sqrt{3}}$.

Chapter 5

Conclusion

In this thesis we have studied spherically- symmetric cosmological models in Einstein-aether theory with a scalar field, whose potential depends on the time-like aether vector field through the expansion and shear scalars. Focusing on the special case of the models where we assume that

$$3c_\theta \equiv c_1 + 3c_2 + c_3 = 0$$

and $a_3 = 0$, leads to a compact phase space. From the evolution equations we obtain a three-dimensional dynamical system in terms of expansion-normalized variables, which we used to simplify our analysis and make it easier to study. We studied these models to find that there always exists a future attractor at some equilibrium points at different values of the parameters $k, c > 0$, and $-\infty < \alpha < \infty$. We found that the only equilibrium points which are sink points are ${}^{+}P_1$,${}^{\pm}P_2$ and ${}^{\pm}P_4$. The main mathematical result we get is that the stability conditions depend on the values of c and k but does not depend on α, which lead to two cases of c.

The first case is when $c < \frac{1}{2}$, we found that ${}^{+}P_2$ and ${}^{\pm}P_4$ are sinks for any values of k. ${}^{+}P_1$ is a sink only for $k > \sqrt{\frac{3}{2}}$ and satisfy the conditions $4c^2 + \frac{3}{2k^2} < 1$, $2 < y^* < \frac{1}{c}\sqrt{1 - \frac{3}{2k^2}}$. Also, ${}^{-}P_2$ is a sink for two different ranges of k. To illustrate this more, when $k < \sqrt{\frac{3}{2}}$ we found ${}^{-}P_2$ is sink when $-2 < y^* < \frac{1}{c}$. On the other hand, when $k > \sqrt{\frac{3}{2}}$ we found it is a sink for two different ranges which are given by $-2 < y^* < -\frac{1}{c}\sqrt{1 - \frac{3}{2k^2}}$ and $\frac{1}{c}\sqrt{1 - \frac{3}{2k^2}} < y^* < \frac{1}{c}$.

The second case is when $c > \frac{1}{2}$: the entire line of ${}^{+}P_2$ is a sink for any value of k. In additions, the entire line of ${}^{-}P_2$ is a sink for $k < \sqrt{\frac{3}{2}}$, while, ${}^{-}P_2$ when $k > \sqrt{\frac{3}{2}}$ is a sink if either one of these conditions satisfied $\frac{1}{c}\sqrt{1 - \frac{3}{2k^2}} < y^* < \frac{1}{c}$ or $-\frac{1}{c} < y^* < -\frac{1}{c}\sqrt{1 - \frac{3}{2k^2}}$. The most interesting result which we found in this thesis

is that P_5 and P_6 are not equilibrium points of the 4 - dimensional dynamical system while they appear to be equilibrium points of the 3 - dimensional dynamical system. After studying the stability for P_5 and P_6 in the 3 - dimensional dynamical system we have found that these points are points where the orbit changes from the positive root of x to the negative root of x or vice-versa.

In summary, we have found that there always exists a future attractor for the points ${}^{+}P_1, {}^{\pm}P_2, {}^{\pm}P_4$ at different values of the given parameters. The analysis for P_7 to P_{10} is taken from [34].

In the future, we recommend additional investigations of the three- dimensional dynamical system, and studying what will happen if c_θ and a_3 are not zero. Moreover, there is one equilibrium point on the boundary of the three dimensional dynamical system which is not in the $V = 0$ invariant set nor in the FLRW set which needs analysis, $Q = \pm 1$, $V = \pm\frac{\sqrt{3}\alpha}{2}$ and $y = \pm\frac{\sqrt{2(2k^2-3)-3k^2\alpha^2}}{2ck}$. In general, in this thesis I have studied the local stability of some of the equilibrium points of the dynamical system corresponding to physical cosmological models.

Bibliography

[1] W. Donnelly and T. Jacobson, *Phys. Rev. D* **82, 064032** (2010).

[2] T. Jacobson and D. Mattingly, *Phys. Rev. D* **64, 024028** (2001).

[3] P. Horava, *Phys. Rev. D* **79, 084008** (2009).

[4] T. Jacobson, *Phys. Rev, D* **81, 081501** (2010).

[5] D. Wiltshire, *Phys. Rev, D* **88, 083529** (2013).

[6] K.A. Olive, *Phys. Rep, D* **190, 308** (1990).

[7] A.D. Linde, *Inflation and quantum cosmology in 300 Years of Gravitation, D* **604-430** (1987).

[8] I. Carruthers and T. Jacobson, *Phys Rev D* **83, 024034** (2011).

[9] S. Kanno and J. Soda, *Phys. Rev. D* **74, 063505** (2006).

[10] T. G. Zlosnik, P. G. Ferreira, and G.D. Starkman, *Phys. Rev D* **75, 044017** (2007).

[11] M. Gasparini, *Phys. Lett. D* **163, 84** (1985).

[12] B. Li, D. F. Mota, and J.D. Barrow, *Phys. Rev. D* **77, 024032** (2008).

[13] J. A. Zuntz, P. G. Ferreira, and T. G. Zlosnik, *Phys. Rev. Lett. D* **101, 261102** (2008).

[14] T. Clifton, P. G. Ferreira, A. Padilla, and C. Skordis, *Modified Gravity and Cosmology.* (2012). arXiv:1106.2476v3.

[15] J.D. Barrow, *phys. Rev. D* **85, 047503** (2012).

[16] E. Cremmer, S. Ferrara, C. Kounnas, and D.V.Nanopoulos, *Phys. Lett, D* **61,133** (1983).

[17] J. Ellis, A.B.Lahanas, D.V. Nanopoulos, and K. Tamvakis, *Phys. Lett, D* **134 ,429** (1984).

[18] A. Salam and E. Sezgin, *Phys. Lett, D* **47 ,147** (1984).

[19] K. Maeda and H. Nishino, *Phys. Lett, D* **154, 358** (1985).

[20] L. J.Romans, *Nucl Phys. D* **269, 691** (1986).

[21] A.R. Liddle, A. Mazumdar, and F.E. Schunck, *Phys. Rev. D* **58, 061301** (1998).

[22] A. A. Coley and R. J. van den Hoogen, *Phys. Rev. D* **62, 023517** (2000).

[23] K. A. Malik and D. Wands, *Phys. Rev. D* **59, 123501** (1999).

[24] E. J. Copeland, A. Mazumdar, and N. J. Nunes, *Phys. Rev. D* **60, 083506** (1999).

[25] A. M. Green and J. E. Lidsey, *Phys. Rev. D* **61, 067301** (2000).

[26] A.P. Billyard, R.J. van den Hoogen, J. Ibañez, and I. Olasagasti, *Class. Quant. Grav. D* **16, 4035** (1999).

[27] E.J. Copeland, A.R. Liddle, and D.Wands, *Phys. Rev.D* **57, 4686** (1998).

[28] R.J. van den Hoogen, A. A. Coley, and D. Wands, *Class. Quant. Grav.* **16, 1843** (1999).

[29] A.P. Billyard, A.A. Coley, and R.J. van den Hoogen, *Phys. Rev.D* **58, 123501** (1998).

[30] A.A. Coley, *Dynamical systems and cosmology*, Kluwer Academic, (2003).

[31] J. Khoury, B. A. Ovrut, P. J. Steinhardt, and N. Turok, *Phys. Rev. D* **64, 123522** (2001).

[32] A. Coley and W. C. Lim, *Class. Quant. Grav.* **22, 3073** (2005).

[33] J. K. Hale, *Dynamics and Bifurcations*, springier, (1991).

[34] A. A. Coley, B.Alhulaimi, G. Leon, and P.Sandin, *Spherical symmetric Einstein-aether Cosmological Models II: Scalar Field".* print paper unpublished.

[35] H. Stephani, D. Kramer, M. A. H. MacCallum, C. A. Hoenselaers, E. Herlt, *Exact solutions of Einstein's field equations, second edition* (Cambridge University Press, Cambridge, 2003).

[36] A. A. Coley, G. Leon, P.Sandin, and J. Latta, *"Spherical symmetric Einstein-aether Cosmological Models II: Perfect Fluid".* (2015). arXiv:1508.00276.